

NTS-1262

SANDIA REPORT

SAND83-0280 • Unlimited Release • UC-70

Printed March 1983

Hydrology of Sealing a Repository in Saturated Tuff

Lisa A. Mondy

Prepared by
Sandia National Laboratories
Albuquerque, New Mexico 87185 and Livermore, California 94550
for the United States Department of Energy
under Contract DE-AC04-76DP00789

HYDROLOGY DOCUMENT NUMBER 153

Issued by Sandia National Laboratories, operated for the United States Department of Energy by Sandia Corporation.

NOTICE: This report was prepared as an account of work sponsored by an agency of the United States Government. Neither the United States Government nor any agency thereof, nor any of their employees, nor any of their contractors, subcontractors, or their employees, makes any warranty, express or implied, or assumes any legal liability or responsibility for the accuracy, completeness, or usefulness of any information, apparatus, product, or process disclosed, or represents that its use would not infringe privately owned rights. Reference herein to any specific commercial product, process, or service by trade name, trademark, manufacturer, or otherwise, does not necessarily constitute or imply its endorsement, recommendation, or favoring by the United States Government, any agency thereof or any of their contractors or subcontractors. The views and opinions expressed herein do not necessarily state or reflect those of the United States Government, any agency thereof or any of their contractors or subcontractors.

Printed in the United States of America
Available from
National Technical Information Service
U.S. Department of Commerce
5285 Port Royal Road
Springfield, VA 22161

NTIS price codes
Printed copy: A04
Microfiche copy: A01

SAND83-0280
Unlimited Release
Printed March 1983

HYDROLOGY OF SEALING A REPOSITORY IN SATURATED TUFF

Lisa A. Mondy
Fluid Mechanics and Heat Transfer Division 1512
Sandia National Laboratories
Albuquerque, NM 87185

ABSTRACT

Hydrologic modeling studies were performed to aid in determining both the need for and design of seals for the drifts and shafts of nuclear waste repositories. It was assumed that the repositories were located in volcanic tuff such as is found in Yucca Mountain at the Nevada Test Site. This modeling study dealt only with repositories in saturated rock and investigated the effects on groundwater flow once drifts and shafts are filled with materials of various permeability. Temperature effects were not examined. Modeling was limited to two dimensions, necessitating simplifying assumptions in some cases. Groundwater flow for the drift model was assumed to be due primarily to a hydraulic head gradient caused by a dipping water table similar to that found in the Yucca Mountain region. In the shaft model a vertical pressure gradient was assumed so that comparisons of sealing designs could be made. Results indicated that observable deviations in the groundwater flow near a repository would occur unless the drifts and shafts were backfilled to a permeability approaching that of the native rock. A series of low permeability blocks in the drifts showed promise in reducing these deviations in groundwater flow, as long as the spacing between blocks remained relatively short (less than ten meters). Sealing only the intersections of drifts proved ineffective. The preferred orientation for the repository appeared to be one with the emplacement drifts perpendicular to the dominant flow direction. This orientation allowed less water to flow past the waste, and the access drifts could be used to provide a path of least resistance to draw

more water away from the emplacement drifts. The most effective measure to prevent large flow rates through vertical shafts was to backfill the shaft to a permeability approaching that of the undisturbed rock. Bulkheads placed in the shaft had little influence on the flow. The effects of a highly permeable disturbed zone 1.37 m in thickness produced by drilling the shaft were also studied. Flow could be discouraged from occurring in this zone by extending grout from the shaft through this zone. However, when the grout was assumed to become more permeable with time, extension of grout into the disturbed zone no longer encouraged deviation of flow away from the disturbed zone.

TABLE OF CONTENTS

	<u>Page</u>
INTRODUCTION.	11
MODELS.	12
ISOLATED DRIFT STUDIES.	16
MULTIPLE DRIFT STUDIES.	19
SHAFT STUDIES	22
SUMMARY AND CONCLUSIONS	26
REFERENCES.	29

ILLUSTRATIONS

<u>Table</u>	<u>Page</u>
1 Material Properties.	30
2 Material Properties Used in Shaft Studies.	31
3 Comparative Flow through Isolated Drifts	32
4 Comparative Flow Rates near a Shaft.	33
5 Comparative Flow Rates near a Shaft with the Enhanced Seal Design as a Function of Time.	34

LIST OF FIGURES

<u>Figure</u>	<u>Page</u>
1 Elements and Boundary Conditions for Isolated Drift Studies	35
2 Elements and Boundary Conditions for Plan View Studies.	36
3 Elements and Boundary Conditions for Shaft Studies.	37
4 Isolated Drift in Saturated Tuff ($k_{rock} = 10^{-15} m^2$) Backfilled with Material ($k_{fill} = 10^{-14} m^2$)	38
5 Isolated Drift in Saturated Tuff ($k_{rock} = 10^{-15} m^2$) Backfilled with Material ($k_{fill} = 10^{-13} m^2$)	39
6 Isolated Drift in Saturated Tuff ($k_{rock} = 10^{-15} m^2$) Backfilled with Little Material ($k_{fill} = 10^{-10} m^2$).	40
7 Isolated Drift in Saturated Tuff ($k_{fill} = 10^{-10} m^2$) with Boundary Conditions Prescribed 200m from Drift.	41
8 Isolated Drift in Saturated Tuff ($k_{fill} = 10^{-10} m^2$) with Boundary Conditions Prescribed 100m from Drift.	41
9 Cross-section of an Isolated Drift ($k_{fill} = 10^{-10} m^2$) Placed Perpendicular to the Flow.	42

LIST OF FIGURES

<u>Figure</u>		<u>Page</u>
10	Flow through a Drift with Three 25m Long, Low Permeability Blocks.	43
11	Flow through a Drift with Eight 25m Long, Low Permeability Blocks.	44
12	Plan View of Vertical Emplacement Repository Section	45
13	Flow through a Repository with the Emplacement Drifts Placed Parallel to the Hydraulic Gradient	46
14	Flow through the Undisturbed Region.	46
15	Flow through a Repository with the Drifts Between Some Pairs of Access Tunnels Backfilled to the Rock Permeability, the Remaining have a Permeability of $10^{-10}m^2$. . .	47
16	Flow through a Repository with Some Emplace- ment Drifts Backfilled to Rock Permeability, while Neighboring Drifts are only Loosely Filled to a Permeability of $10^{-10}m^2$	47
17	Flow through a Repository with Junctions between Drifts and Access Tunnels Backfilled to Rock Permeability	48
18	Flow through a Repository with 4.0 Meter Blocks of Rock Permeability Spaced 4.0 Meters Apart	48
19	Flow through a Repository with Blocks in an Emplacement Drift while a Neighboring Drift is only Loosely Backfilled.	49
20	Flow through a Repository with 4.0 Meter Blocks Spaced 16 Meters Apart.	49
21	Flow through a Repository Positioned so that the Dominant Flow is Parallel to the Access Drifts.	50

LIST OF FIGURES

<u>Figure</u>		<u>Page</u>
22	Shaft Studies.	51
23	Vertical Flow through Undisturbed Rock	52
24	Vertical Flow near a Shaft with Minimal Seal, Backfill of Permeability $10^{-13}m^2$	53
25	Vertical Flow near a Shaft with Minimal Seal, Backfill of Permeability $10^{-16}m^2$	54
26	Vertical Flow near a Shaft with a Clay and a Concrete Bulkhead in a Backfill of Permeability $10^{-16}m^2$	55
27	Enhanced Seal Design	56
28	Flow near a Shaft with the Enhanced Seal Design; Main Shaft Backfilled to Permeability $10^{-13}m^2$	57
29	Flow near a Shaft with the Enhanced Seal Design; Main Shaft Backfilled to Permeability $10^{-16}m^2$	58
30	Flow near a Shaft with the Enhanced Seal Design, after 300 Years.	59
31	Flow near a Shaft with the Enhanced Seal Design, after 3000 Years	60
32	Constant-Pressure Lines for Flow near a Shaft with the Enhanced Seal Design; Constant- Pressure Boundary Conditions along Top and Bottom Boundaries.	61
33	Constant-Pressure Lines for Flow near a Shaft with the Enhanced Seal Design; The Top Boundary is Constant Pressure and the Bottom is Constant Flow.	62
34	Streamlines near a Shaft with the Enhanced Seal Design; The Top Boundary is Constant Pressure and the Bottom is Constant Flow	63

SYMBOLS

A	cross-sectional area of solid and pores
g	gravity acceleration
\tilde{k}	intrinsic permeability tensor
p	pressure
Q	flowrate
v_0	superficial velocity (Q/A)
v_i	components of superficial velocity
x,y,z	components of direction
μ	fluid viscosity
ϕ	hydraulic head
ρ	density of fluid
ψ	stream function

INTRODUCTION

One of the most promising approaches to the problem of high-level radioactive waste disposal is to place the waste in continental geologic environments such as rock formations underground. Yucca Mountain at the Nevada Test Site (NTS) is being studied in the Nevada Nuclear Waste Storage Investigations (NNWSI) Project, managed by the Nevada Operations Office of the U. S. Department of Energy, as a possible waste repository site of this type. There is concern with any underground site that leaching may occur, allowing radionuclides to be carried by the groundwater to the biosphere. Therefore, an understanding of the hydrology of the region and the effects of mining and emplacing waste is needed. As part of ongoing work funded by the NNWSI Project, we have carried out a set of hydrological calculations to aid in understanding the effects of repository construction and orientation on groundwater flow. These calculations are in the form of parameter studies, performed primarily to aid in assessing the need for and the design of repository seals. We examine both drifts and shafts in this preliminary study.

The finite element code MARIAH can be used to describe two-dimensional, incompressible, Darcy flow through saturated porous media [1]. In this study it has been used as a computational tool to estimate the effects on the groundwater flow of shafts and drifts backfilled with a material generally of

higher permeability than that of the native rock. Although MARIAH has the capability to couple heat and mass flow, this study is limited to isothermal modeling. Effects due to heat generation by the waste canisters are not considered.

The first part of the study investigates the effects on groundwater flow that result from backfilling a single drift with material of higher permeability (lower resistance to flow) than that of the surrounding native rock. The influence of the orientation of the drift with respect to the dominant flow direction as well as the influence of the prescribed boundary conditions are evaluated. The effectiveness of low permeability blocks in lessening perturbations to the original, undisturbed, flow field is explored also. We then investigate the effects of orientation and various sealing schemes for a network of drifts.

Finally, we examine the changes in groundwater flow that result from placing a shaft in a region with an assumed vertical flow field. MARIAH is used to evaluate various seal designs for this shaft.

MODELS

Darcy's law states that the superficial velocity (v_o) is proportional to the driving gradient:

$$v_o = \frac{-k}{\mu} (\nabla P - \rho g) \quad , \quad (1)$$

where k is the intrinsic solid permeability tensor, μ is the

fluid viscosity, ∇P is the pressure gradient, ρ is the fluid density and g is the acceleration due to gravity [2]. The superficial velocity is the volume rate of flow through a unit cross-sectional area of the solid plus the fluid. Note that at any particular point the superficial velocity is not the true fluid velocity in the porous matrix.

A useful tool of fluid mechanics is the stream function $\phi(x,y)$, defined by the equations

$$v_x = - \frac{\delta\phi}{\delta y} \quad \text{and} \quad v_y = \frac{\delta\phi}{\delta x} \quad , \quad (2)$$

where v_x and v_y are the superficial velocity components. The curves $\phi = \text{constant}$ are the streamlines or flow paths. As an aid to visualizing the flow, the results of many calculations are given as streamline plots. The difference between two stream functions gives a volumetric flow rate per unit width. When streamlines which increase uniformly in value are plotted, the distance between streamlines is indicative of the superficial velocity in that region; the closer together the streamlines the faster the flow.

The material properties used in this study are listed in Table 1. Los Alamos Technical Associates (LATA) provided typical sealing material permeabilities and rock permeabilities, listed in Table 2, used for the shaft studies. Although the single drift studies are purely hypothetical, the permeability of the host rock was chosen as typical of the Yucca Mountain region [4]. The plan view studies use the dimensions and configurations

of the drifts proposed for the vertical emplacement scheme, outlined in Reference 3. The horizon for the plan view studies is assumed to be at a depth of 420 meters in the Topopah Springs member of the Paintbrush Tuff. Peters [4] is the source of the rock permeability for this horizon.

The code MARIAH models flow in saturated regions only. Although the Topopah Springs member is in the partially saturated zone, these preliminary studies treat it as if it were saturated. Similar studies can and will be done with the code SAGUARO [5], which is being developed to describe flow in partially saturated zones.

This study ignores the effect of the heat generated by the waste canisters. We do not imply that the free convection term due to this heat will always be negligible. The approach is to initially decouple mass and heat transfer and determine the magnitude of the forced convection term alone. All results described here are steady-state solutions. Steady state typically is reached within five years for the permeabilities and geometries used in these studies.

Figure 1 shows the element grid and the boundary conditions used in the horizontal drift studies. The drift resides in the thin line of elements located in the center of the grid. The boundary conditions correspond to prescribing a driving gradient in the horizontal direction and no-flow conditions at the top and bottom of the finite element grid. The hydraulic gradient is assumed to range from 0.0025 m/m to 0.25 m/m. At the left

and right boundaries, it is assumed that no vertical flow occurs. The constant hydraulic head at these boundaries is given by

$$\phi = \rho g (\phi + z) \quad , \quad (3)$$

where $\phi = P/\rho g$, the pressure head. The top and bottom boundaries are assumed to be no-flow boundaries and are set far enough away from the disturbed region so that they do not affect the flow near the drift.

Figure 2 shows the element grid and boundary conditions for studies of the network of access tunnels and storage drifts shown in plan view in Figure 12. Again the left and right boundaries are assumed to have a constant hydraulic head. The top and bottom boundaries are lines of symmetry. Since forces will be equal across these lines, no fluid can cross them.

A similar approach was used in studies of seals for vertical shafts. Figure 3 shows the element grid and boundary conditions used in these cases. The shaft and its associated disturbed zone are located in the smaller elements near the left boundary. An axisymmetric geometry is assumed, along a vertical section consisting of one type of tuff. The left (radius = 0) boundary is a line of symmetry and the right (radius = 45.72 m) boundary is set far enough away so that it does not affect the flow. The region is assumed to have a superimposed, vertical, pressure gradient. A lower boundary of constant flow instead of constant pressure is used in one case to illustrate how the boundary condition affects the behavior of the flow.

Since MARIAH presently is limited to two-dimensional geometry, the hydrologic models are two-dimensional approximations to three-dimensional problems. The significance of these approximations is discussed for the individual cases.

ISOLATED DRIFT STUDIES

Initial calculations have been done to estimate the groundwater flow in the area adjacent to a hypothetical, 5m high by 7m wide by 450m long, isolated drift. The rock surrounding the drift is assumed to have constant properties and the drift to be backfilled with material of permeability several orders of magnitude higher than that of the rock. With a rock permeability of 10^{-15} m^2 (the approximate mean permeability of the saturated, Yucca Mountain strata), observable deviations in the undisturbed streamlines occur unless the backfill permeability is within an order of magnitude of the rock permeability. Figures 4 through 6 show the steady-state streamlines in three examples of groundwater flow with a drift parallel to the hydraulic head gradient. The permeability of the backfill increases from 10^{-14} m^2 in Figure 4, to 10^{-13} m^2 in Figure 5, to 10^{-10} m^2 (simulating little or no fill) in Figure 6. The value of the maximum volumetric flow rate through the drift for each case is listed in Table 3. The flow rate is calculated through the cross section in a drift where the maximum superficial velocity occurs. Note that the flow rate for the third entry and the seventh entry in Table 3 are the same although the permeability of the drift is increased by a

factor of 30. This implies that a difference of four orders of magnitude in permeability between the rock and the backfill behaves as an infinite difference; it simulates no backfill.

Calculations have been done with values of 0.0025 and 0.25 m/m for the driving gradient. The streamline plots remain similar, but the value of the flow rate increases with increasing head differential. It is obvious from looking at Darcy's law for incompressible fluids, that in one-dimensional flow, given the flow rate at one head differential one can calculate the flow rate at any other by simple scaling, assuming that the rock and fluid properties are constant and homogeneous.

Note that the boundary conditions at the top and bottom surfaces of the problem affect the streamlines. In Figures 4 through 6 the distance from the drift to either horizontal surface is 400 meters. Figures 7 and 8 show the same case as Figure 6; however, the distance from the drift to the horizontal boundary is only 200 and 100 meters, respectively. The streamlines are forced to be parallel to the boundary at the boundary by the no-flow condition. Even with a distance of 400 meters as in the first three figures, the boundary may be affecting the results, but to a much lower degree. As the strata thicknesses in Yucca Mountain are always less than 800 meters, the actual strata dimensions and permeabilities could also change the flow pattern. In the calculations illustrated in Figures 4 through 6, the left and right boundaries are 400 meters from the

ends of the drift. The assumption of no vertical flow at the left and right boundaries does not appear to affect the solution significantly, even when the boundaries are placed only 100 meters from the ends of the drift as in Figures 7 and 8.

It must be kept in mind that Figures 4 through 8 are two-dimensional representations for three-dimensional problems. In each calculation the "drift" is a semi-infinite plane extending perpendicularly out from the plane of the paper. The flow rates listed in Table 1 are calculated from a two-dimensional representation of the three-dimensional problem, since the rock on either side of the drift would also affect the flow. The flow rate values can only be regarded as bounding values or compared qualitatively to each other.

Figure 9 shows the crossflow streamlines for a drift positioned so that it is perpendicular to the driving gradient. This is an accurate representation of the flow over the center of a long drift where end effects are not important. Very little change in the streamlines can be seen beyond a few meters from the drift.

Figures 10 and 11 show the effects of placing 25 m long blocks of low permeability (within an order of magnitude of that of the rock) in an otherwise open drift. If flow were strictly one-dimensional and horizontal, Darcy's law could be written

$$v_0 = - \left[\sum_{i=1}^n \frac{x_i}{k_i} \right]^{-1} \Delta P \quad (4)$$

where X_i is the distance through material of permeability k_i , and n is the number of materials, and ΔP is the pressure drop. Each drift in Figures 10 and 11 would have a total resistance to flow the same as a homogeneous material of permeability 10^{-14} m^2 . In other words, the superficial velocity through the drift would be the same as the velocity through the drift in Figure 4, given the same pressure gradient; however, the flow is obviously not one-dimensional. The geometry and spacing of the blocks affect the streamlines and flow rate. As the distance between the blocks decreases, the seriousness of the perturbations in flow also decreases. For the case shown in Figure 10, the maximum flow rate in the drift is $2.6 \times 10^{-8} \text{ m}^3/\text{s}$, while for that in Figure 11, the maximum flow rate is $8.3 \times 10^{-9} \text{ m}^3/\text{s}$. The maximum flow for the same problem, but with the homogeneous backfill of Figure 4, is $4.7 \times 10^{-9} \text{ m}^3/\text{s}$.

MULTIPLE DRIFT STUDIES

We also investigated the effect on groundwater flow due to multiple drifts. We used a two-dimensional plan view, assuming that there are negligible effects from flow in the third (vertical) direction. Figure 12 depicts a section in the center of a grid of access and emplacement drifts. Geometrically, all boundaries are lines of symmetry, as the grid extends to all sides. The emplacement drifts and access tunnels are labeled in the figure.

If the predominant hydraulic gradient, superimposed in the third dimension, is assumed to be parallel to the emplacement drifts, the fluid follows the path of least resistance. The majority of the flow is through the emplacement drifts if the drifts have not been backfilled to a permeability approaching that of the surrounding rock. In Figure 13, both access and emplacement drifts are assumed to have a permeability approximately four orders of magnitude greater than the native rock. Ten streamlines are concentrated in each emplacement drift. Recall that the same flow rate occurs between contiguous streamlines, so that in Figure 13 approximately ten times the amount of liquid flows in the drift as flows in the same plane in the rock above the drift. The streamlines also show that the presence of the access drifts has little effect on the flow. For comparison, Figure 14 shows the streamlines through the same region before mining drifts.

Figure 15 illustrates the case in which emplacement drifts are backfilled to the permeability of the native rock. The permeability of the access tunnels and the emplacement drifts to the left and right of the tunnels is four orders of magnitude greater than that of the native rock. The flow quickly spreads out when the fluid reaches the backfilled region and just as quickly returns to the drifts downstream. Figure 16 shows the fluid's dominant path when only one drift is tightly backfilled to the permeability of the host rock. The access tunnels become the fluid's dominant path.

Another idea for sealing is to place low permeability blocks at the ends of loosely backfilled emplacement drifts. Figure 17 shows the futility of such a simple seal; the fluid is discouraged for about 5 meters from its path through the drifts.

Next, a series of blocks similar to that used in the isolated drift study above is tested as a sealing system. Figures 18 and 19 illustrate the streamlines corresponding to the case in which both drifts are filled with blocks four meters in width and spaced four meters apart and to the case in which alternating drifts are filled with the blocks, respectively. Again the remaining drifts and tunnels are backfilled to a permeability four orders of magnitude greater than the rock permeability. Note that the blocks are successful in causing the groundwater flow to be diverted from the block-filled drift into the loosely filled drift. The streamlines in Figure 20 are calculated for the situation of sealing the drifts with four meter wide blocks spaced 16 meters apart.

Figure 21, the last illustration in the plan view series, shows the result of placing the hydraulic gradient perpendicular, rather than parallel, to the emplacement drifts. All drifts and tunnels are backfilled to a permeability approximately four orders of magnitude greater than that of the native rock. As is expected, the flow occurs primarily through the access tunnels, although the emplacement drifts show some effect on the path, causing approximately 40% of the fluid to detour up

to 25 m into the emplacement drifts but again to return within 5 m downstream.

SHAFT STUDIES

We have modeled four hypothetical cases for flow near a vertical shaft. Figure 22 shows the geometry of all the cases [6]. Table 2 lists the materials used and their properties during three time periods. The first time period is from zero to 300 years, the second from 300 to 3000 years and the third from 3000 to 30,000 years.

The flow rate through undisturbed rock in a circular cross-sectional area of radius 45.72 m can be calculated with Darcy's law. For a pressure head gradient ($\partial\phi/\partial z$) of 0.01 m/m, through rock with a permeability of $3.3 \times 10^{-16} \text{ m}^2$, water flows with a volumetric rate of

$$\begin{aligned}
 Q &= v_o \cdot A = \frac{\Delta P / \rho g}{\Delta z} \frac{\rho g k}{\mu} \cdot A & (5) \\
 &= \frac{(.01) \left(1000 \frac{\text{kg}}{\text{m}^3}\right) \left(9.8 \frac{\text{m}}{\text{s}^2}\right) \left(3.3 \times 10^{-16} \text{m}^2\right) \cdot \pi (45.72)^2 \text{m}^2}{\left(9.82 \times 10^{-4} \frac{\text{kg}}{\text{m} \cdot \text{s}}\right)} \\
 &= 2.16 \times 10^{-7} \frac{\text{m}^3}{\text{s}}
 \end{aligned}$$

This situation, with no modifications to the natural rock, corresponds to the first case in the shaft study, the undisturbed case. Figure 23 illustrates 14 streamlines equally

spaced between the smallest and largest value calculated for the region. Recall that each region between contiguous streamlines contains the same amount of flow. The axisymmetric geometry causes the streamlines to become closer together as the radius, and hence the area represented in the figure, increases.

A minimal seal is described as the same region with a loosely backfilled shaft. The shaft is 1.37 meters in radius, with grout extending 0.46 meters beyond the shaft walls. Because of the drilling, a disturbed zone extending 1.37 meters beyond the grout is assumed. The shaft is backfilled with crushed tuff of permeability 10^{-13} m^2 . Note that this backfill is several orders of magnitude more permeable than the native rock. Figure 24 shows the streamlines calculated for this situation. Streamlines appear in the backfilled region and in the disturbed zone, illustrating that much more flow is occurring in the vicinity of the shaft. In Figure 25 the same geometry is illustrated, but the backfill consists of crushed tuff and clay having a permeability within an order of magnitude of the native rock's. The streamlines have shifted away from the shaft, compared to Figure 24, but still more flow occurs near the shaft than in the undisturbed region.

In the next case a more elaborate sealing system is considered. Two large cylindrical blocks, one of clay and the other of concrete, are located along the axis of the shaft and protrude radially into the disturbed zone as keyways. These

bulkheads are 2.44 meters long and extend radially 2.29 meters from the axis. Figure 26 shows that these blocks have little effect on the flow when the tight backfill is used.

An enhanced sealing design is illustrated in Figure 27. Grout extends 1.83 meters beyond the keyways and past the edge of the disturbed zone. With the loose backfill the streamlines are shown in Figure 28. Figure 29 illustrates the situation with tight backfill. It appears that extending the less permeable grout into the disturbed zone has a much greater effect on the flow in the vicinity of the seal than the addition of the bulkheads alone.

Table 4 is a summary of the flow rate results for the first time period. Obviously, when there are more regions of high permeability, more flow will occur, given a fixed pressure gradient. Backfilling the shaft to nearly the permeability of the undisturbed rock does much to reduce the increase in flow caused by the presence of the shaft. The disturbed zone allows a large percentage of the flow to occur in the vicinity of the shaft. Adding the regions of low permeability, such as additional grout, in the disturbed zone helps somewhat to limit the flow through the disturbed zone.

Some sealing materials break down with time, however. In Table 5 the flow rates from the cases with crushed tuff and clay as the shaft backfill are listed for the three time periods. Figures 30 and 31 show the streamlines for the enhanced seal design as the concrete and grout increase in permeability.

As a cross-check, LATA solved some of these cases with a USGS two-dimensional finite-difference code. The results were similar to those listed here [6].

We do not believe that the waste heat in the repository below will produce a steady vertical pressure gradient through the time periods studied. The constant-pressure boundary condition is used merely to make conservative comparisons in the flow fields in the various cases. To illustrate how the boundary condition affects the calculated streamlines, one can calculate the streamlines produced when the bottom boundary is assumed to have constant flow across it rather than having a constant pressure. Figure 32 shows constant-pressure lines for the enhanced seal design with the tight backfill as described earlier with the streamlines in Figure 29. Figure 33 shows constant-pressure lines when the bottom boundary is assumed to have constant flow across it. The flow rate assumed at the bottom boundary is the flow that would occur in the undisturbed region described in Equation 4. Since Darcy's law states that the flow is proportional to the product of the driving gradient and the permeability, forcing materials of different permeability to experience the same pressure drop (as in the shaft cases described above) forces much more fluid through the materials of higher permeability. On the other hand, we force the pressures to differ when we assume that at some arbitrary line (such as the bottom boundary) materials of different permeabilities transmit the same flow rate. The actual physical

situation lies between these two extreme bottom boundary conditions. Figure 34 illustrates the calculated streamlines that occur with the constant-flow boundary condition.

SUMMARY AND CONCLUSIONS

A general premise upon which the effectiveness of drift and shaft seals can be judged, is that the drifts and shafts should be sealed so that the groundwater flow rates and flow patterns approach those occurring in the natural, undisturbed environment. Through a series of parameter studies on a hypothetical, isolated drift surrounded by homogeneous rock, we have looked at the effectiveness of backfill of various permeabilities and of a series of low permeability blocks in diverting flow. Significant deviations to the original flow field occur unless the drift permeability approaches within an order of magnitude of the permeability of the surrounding rock. Blocks of low permeability material placed in the drift show promise of limiting the flow through the drift even when the spaces between blocks are filled only minimally. The greater the number of blocks or the smaller the distance between blocks, the better the ability to divert the flow.

Groundwater flow is most affected when the drifts are positioned parallel to the primary direction of flow. A long region of high permeability allows more flow to be diverted from the less permeable native rock. Placing highly permeable drifts crosswise to the flow influences the flow path very

little. This leads to the conclusion that the preferred orientation of the storage drifts may be perpendicular to the dominant, natural, water flow.

Using a plan view geometry, we have illustrated these conclusions again. It is clear from the plots of streamlines that the fluid will follow the path of least resistance, even traveling up one access tunnel, across an open emplacement drift and down the next access tunnel if every other emplacement drift is backfilled. If only the ends of the drifts are blocked and a large area of high permeability behind the barricade is ignored, the groundwater is not discouraged from flowing through the material of high permeability. Again a series of closely spaced blocks of low permeability manifests the ability to divert some flow from the drifts.

Directional control of groundwater flow may be desired and possibly can be accomplished by orienting the access tunnels parallel to the predominant groundwater flow. It may be appropriate to fill the access tunnels with material of comparatively high permeability relative to the host rock to encourage flow through these tunnels rather than through the emplacement drifts. Recall, however, that the calculations presented are only appropriate for modeling saturated media.

The effects of a disturbed zone with lower resistance to flow is illustrated in the studies of vertical shafts (this disturbed zone is ignored in the drift studies). Simple sealing concepts are analyzed by calculating flow rates through an

affected area assuming a steady pressure gradient. Again, assuming that the most desirable result is to change the natural flow path little, it appears to be best to limit the extent of the disturbed zone as much as possible and to backfill the shaft with material of permeability similar to that of the native rock. Addition of bulkheads has little effect if the shaft itself is backfilled to a permeability approaching that of the host rock.

The limitations of the models to simulate the actual non-isothermal, three-dimensional, physical situations and the fact that the calculations presented are for steady-state flow through saturated porous media should be kept in mind. However, the trends indicated by these calculations can help in the comparison of various sealing approaches, and the results have pointed out some broad principles important in the evaluation of proposed waste repositories in the saturated zone.

ACKNOWLEDGEMENT

Discussions with Rodney Wilson were invaluable in completing this work. I would like to express my appreciation for his help.

REFERENCES

1. Gartling, D. K. and C. E. Hickox, "MARIAH--A Finite Element Computer Program for Incompressible Porous Flow Problems: Users' Manual," SAND79-1623(Revised), September 1982.
2. Bear, J., Dynamics of Fluids in Porous Media, American Elsevier, New York, 1972.
3. Scully, L. W., Memo to J. W. Nunziato, D. F. McVey, and R. D. Krieg dated August 11, 1982, Subject: Engineering Studies to Determine a Nuclear Waste Emplacement Scheme.
4. Peters, R. R., Memo to T. Brandshaug (Re/Spec, Inc.) dated June 15, 1982, Subject: Far-field Thermomechanical Calculations for Four Average Property Cases.
5. Eaton, R. R., D. K. Gartling, and D. E. Larson, "SAGUARO--A Finite Element Computer Program for Partially Saturated Porous Flow Problems," SAND82-2772, July, 1982.
6. U.S. Department of Energy, "Nevada Nuclear Waste Storage Investigations -- Quarterly Report for July-September 1982," NVO-196-32, 1983 (to be published).

Table 1. Material Properties

Density of water (ρ)	1000 kg/m ³
Viscosity of water (μ)	9.82 x 10 ⁻⁴ kg/m•s
Permeability of rock (k_{rock})	1 x 10 ⁻¹⁵ m ² (single drift studies) to 8 x 10 ⁻¹⁵ (multiple drift/ plan view studies)
Permeability of backfill (k_{fill})	variable

Table 2. Material Properties Used in Shaft Studies*

<u>Material</u>	Permeability (m^2) in vertical (z) and horizontal (r) directions (k_z/k_r)		
	Period 1 (0 - 300 years)	Period 2 (300 - 3,000 years)	Period 3 (3,000-30,000 years)
Undisturbed tuff	$3.3 \times 10^{-16}/1 \times 10^{-15}$	$3.3 \times 10^{-16}/1 \times 10^{-15}$	$3.3 \times 10^{-16}/1 \times 10^{-15}$
Disturbed zone tuff	$1 \times 10^{-14}/1 \times 10^{-14}$	$1 \times 10^{-14}/1 \times 10^{-14}$	$1 \times 10^{-14}/1 \times 10^{-14}$
Crushed tuff & clay	$1 \times 10^{-16}/1 \times 10^{-16}$	$1 \times 10^{-16}/1 \times 10^{-16}$	$1 \times 10^{-16}/1 \times 10^{-16}$
Crushed tuff	$1 \times 10^{-13}/1 \times 10^{-13}$	$1 \times 10^{-13}/1 \times 10^{-13}$	$1 \times 10^{-13}/1 \times 10^{-13}$
Clay bulkhead	$1 \times 10^{-17}/5 \times 10^{-17}$	$1 \times 10^{-17}/5 \times 10^{-17}$	$1 \times 10^{-17}/5 \times 10^{-17}$
Reinforced concrete	$1 \times 10^{-17}/1 \times 10^{-17}$	$1 \times 10^{-15}/1 \times 10^{-15}$	$1 \times 10^{-13}/1 \times 10^{-13}$
Grout	$1 \times 10^{-16}/1 \times 10^{-16}$	$1 \times 10^{-13}/1 \times 10^{-13}$	$1 \times 10^{-13}/1 \times 10^{-13}$

*Provided by Los Alamos Technical Associates

Table 3. Comparative Flow through Isolated Drifts*

<u>Case</u>	<u>Figure No.</u>	<u>Permeability of backfill (m²)</u>	<u>Head gradient (m/m)</u>	<u>Maximum Volumetric Flow (m³/s)</u>
1	4	1 x 10 ⁻¹⁴	.0025	4.7 x 10 ⁻⁹
2	5	1 x 10 ⁻¹³	.0025	2.2 x 10 ⁻⁸
3	6	3 x 10 ⁻¹⁰	.0025	3.6 x 10 ⁻⁸
4	4	1 x 10 ⁻¹⁴	.25	4.5 x 10 ⁻⁷
5	5	1 x 10 ⁻¹³	.25	2.1 x 10 ⁻⁶
6	6	3 x 10 ⁻¹⁰	.25	3.5 x 10 ⁻⁶
7	-	1 x 10 ⁻¹¹	.0025	3.6 x 10 ⁻⁸
8	10	block = 1.7x10 ⁻¹⁵ , fill = 1 x 10 ⁻¹⁰	.0025	2.6 x 10 ⁻⁸
9	11	block = 5 x 10 ⁻¹⁵ , fill = 1 x 10 ⁻¹⁰	.0025	8.3 x 10 ⁻⁹

*Surrounding rock permeability = 10⁻¹⁵m²

Table 4. Comparative Flow Rates near a Shaft

Case	Description	Flow Rate, m ³ /sec 32.18m ² *	Flow Rate, m ³ /sec 6566.93m ² **	Percentage of Total Flow Through Disturbed Zone (6.4m Diameter)
1	Undisturbed	1.06 x 10 ⁻⁹	2.16 x 10 ⁻⁷	0.49
2a	Minimal Seal - Crushed Tuff	8.07 x 10 ⁻⁸	2.96 x 10 ⁻⁷	27
2b	Minimal Seal - Crushed Tuff and Clay	2.17 x 10 ⁻⁸	2.37 x 10 ⁻⁷	9.2
3	Preliminary Design - Crushed Tuff & Clay	2.12 x 10 ⁻⁸	2.36 x 10 ⁻⁷	9.0
4a	Enhanced Design - Crushed Tuff	3.03 x 10 ⁻⁸	2.34 x 10 ⁻⁷	13
4b	Enhanced Design - Crushed Tuff & Clay	1.45 x 10 ⁻⁸	2.25 x 10 ⁻⁷	6.4

*Represents the cross-sectional area of a cylinder with a 3.20m radius. The 3.20m radius represents the extent of the disturbed zone.

**Represents the cross-sectional area of a cylinder with a 45.72m radius.

Table 5. Comparative Flow Rates near a Shaft with the Enhanced Seal Design as a Function of Time

<u>Time Period</u>	<u>Flow Rate (m³/sec) 32.18m²*</u>	<u>Flow Rate (m³/sec) 6566.93m²**</u>	<u>Percentage of Total Flow Through Disturbed Zone (6.4m Diameter)</u>
0-300 yrs	1.45 x 10 ⁻⁸	2.25 x 10 ⁻⁷	6.4
300-3000 yrs	6.44 x 10 ⁻⁸	2.78 x 10 ⁻⁷	23
3000-30,000 yrs	6.68 x 10 ⁻⁸	2.83 x 10 ⁻⁷	24

34

*Represents the cross-sectional area of a cylinder with a 3.20m radius. The 3.20m radius represents the extent of the disturbed zone.

**Represents the cross-sectional area of a cylinder with a 45.72m radius.

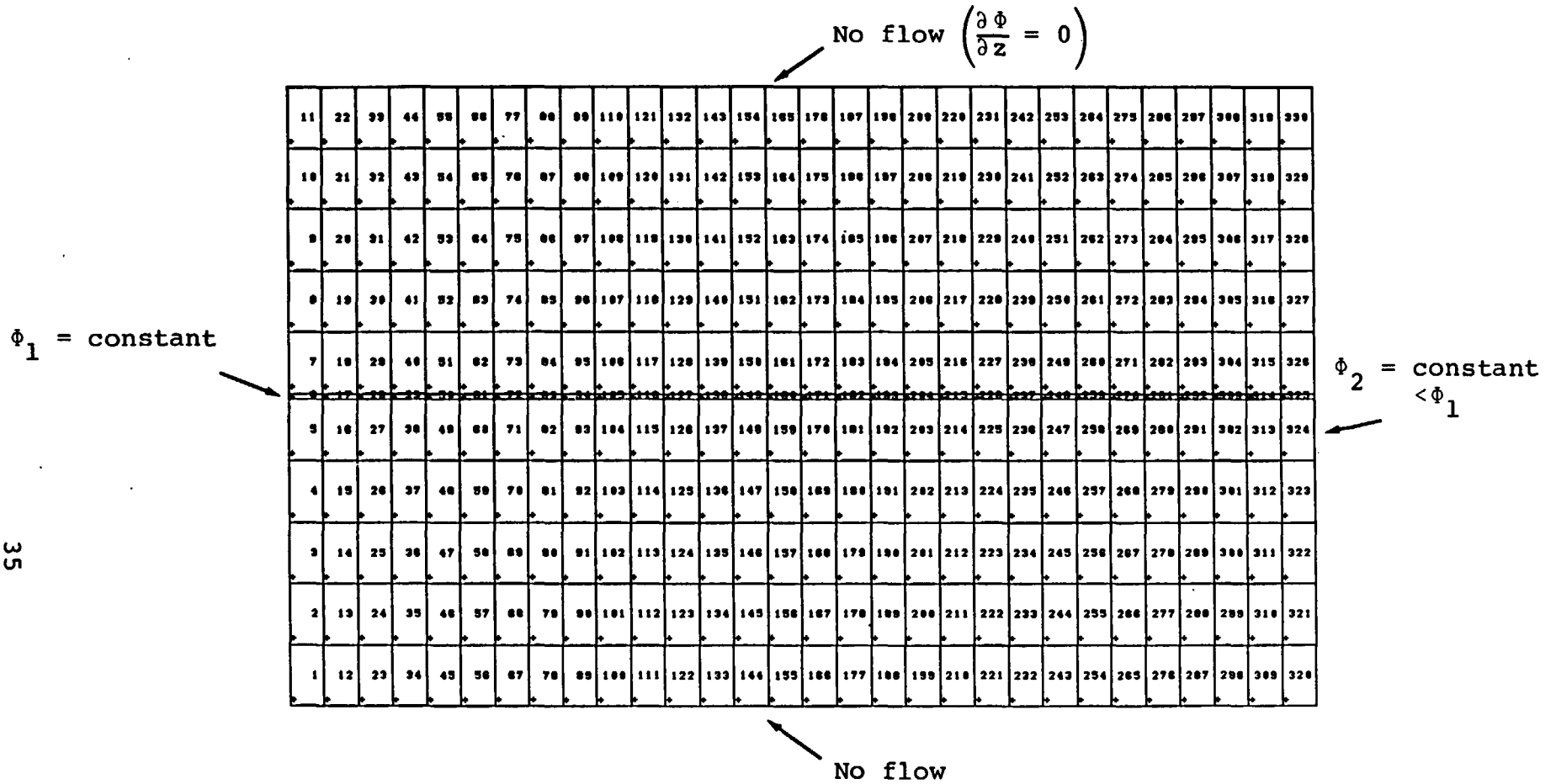


Figure 1. Elements and boundary conditions for isolated drift studies.

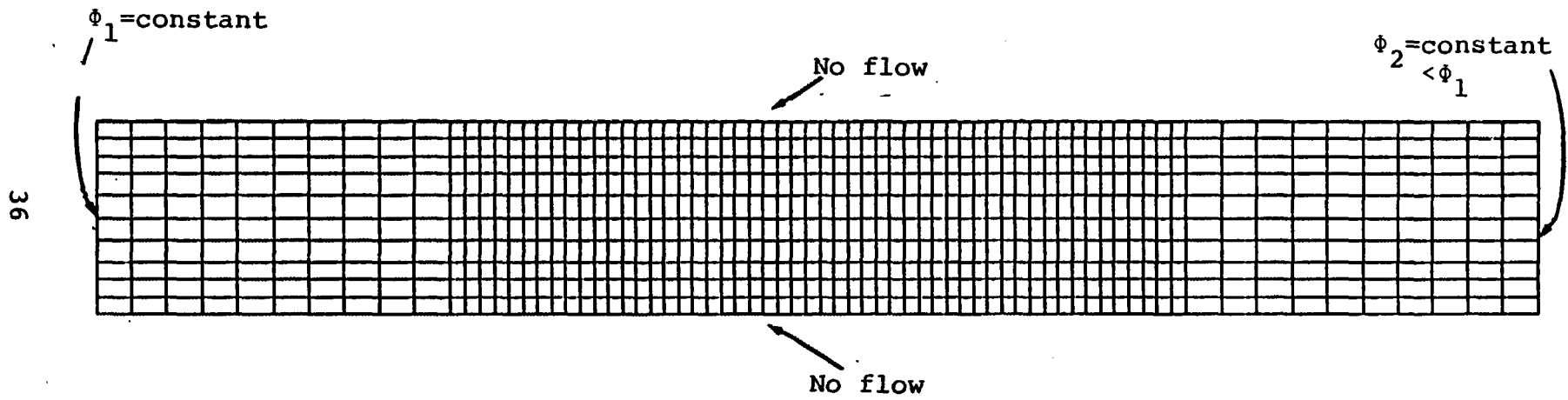


Figure 2. Elements and boundary conditions for plan view studies.

$P/\rho g = \text{constant}$

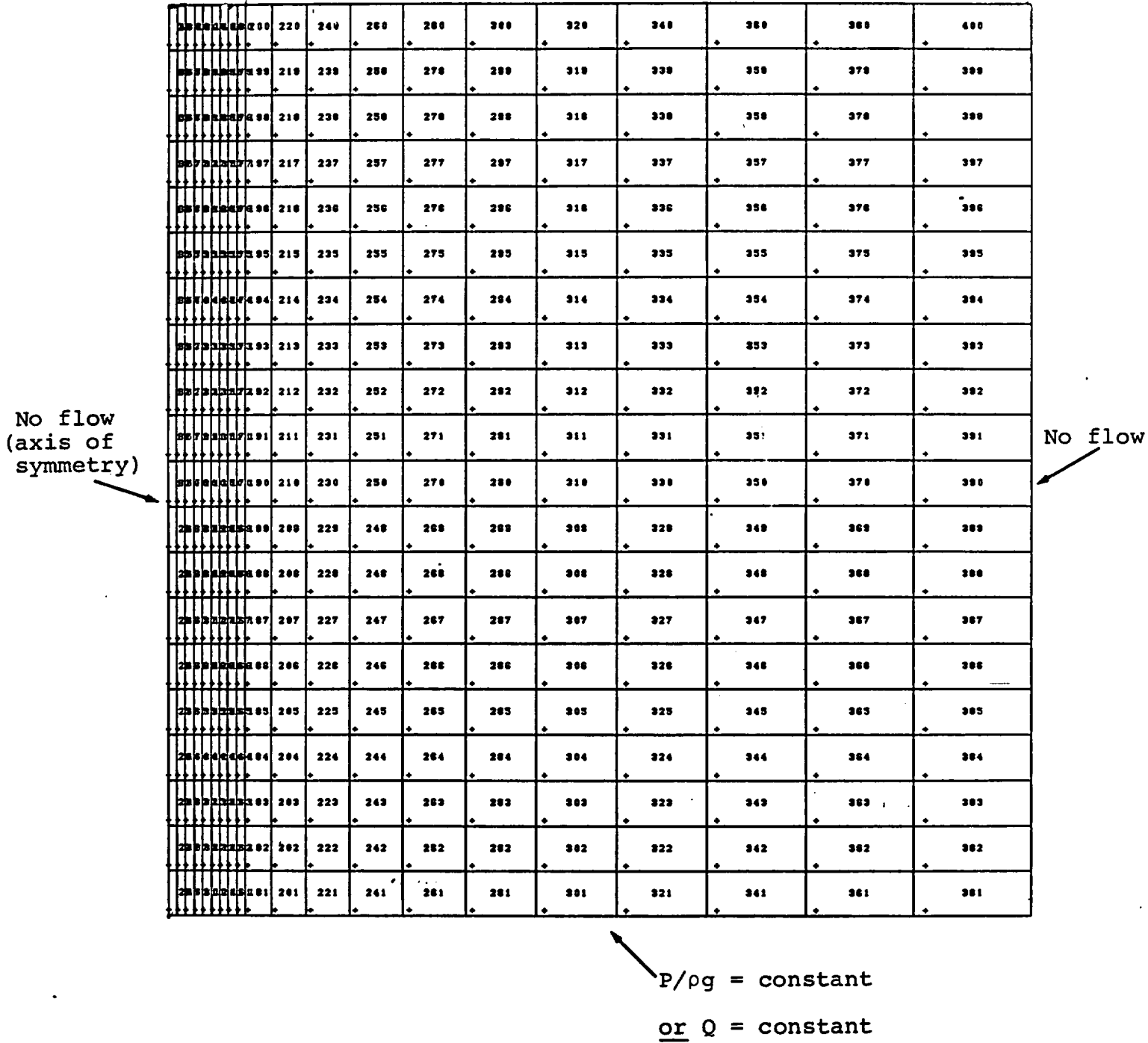


Figure 3. Elements and boundary conditions for shaft studies.

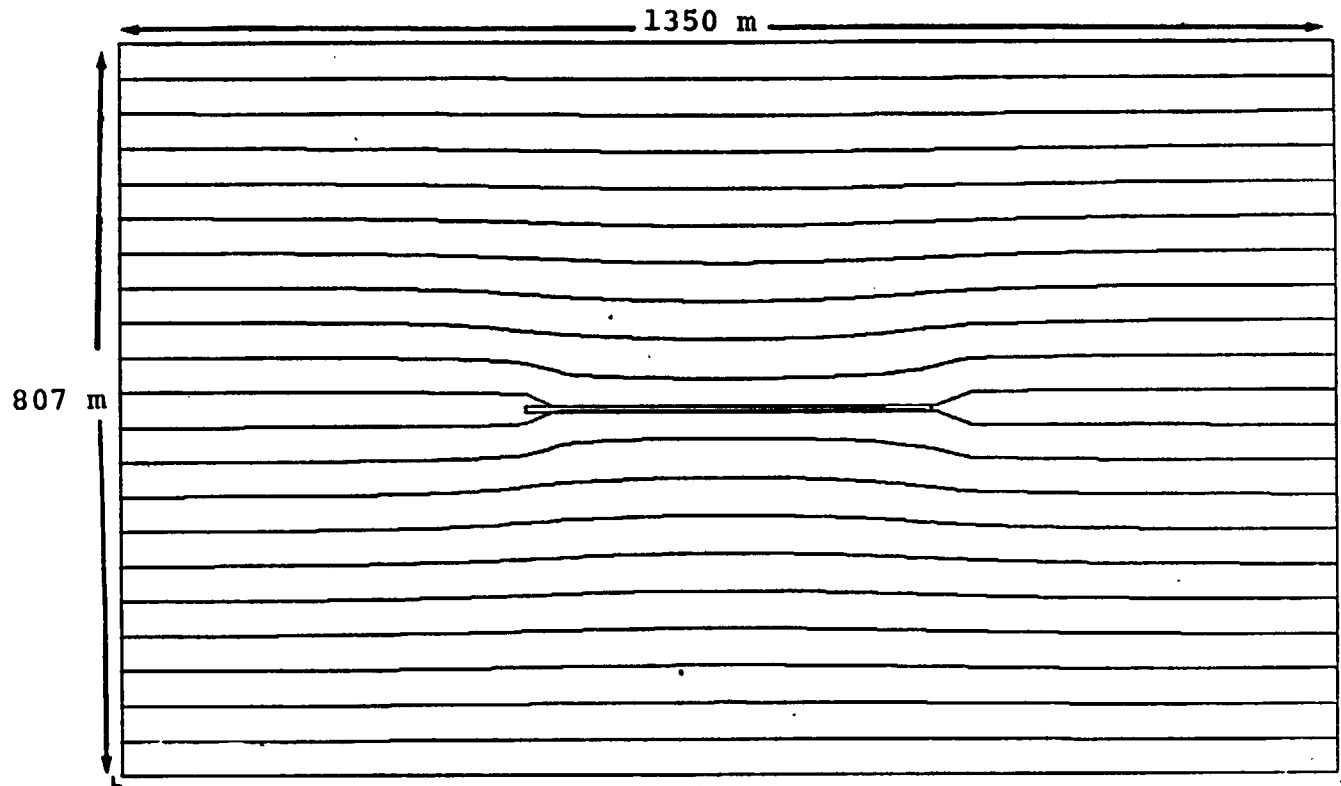


Figure 4. Isolated drift in saturated tuff ($k_{\text{rock}} = 10^{-15} \text{ m}^2$) backfilled with material ($k_{\text{fill}} = 10^{-14} \text{ m}^2$). Lines are evenly spaced streamlines resulting when a constant hydraulic gradient is held from left to right boundaries.

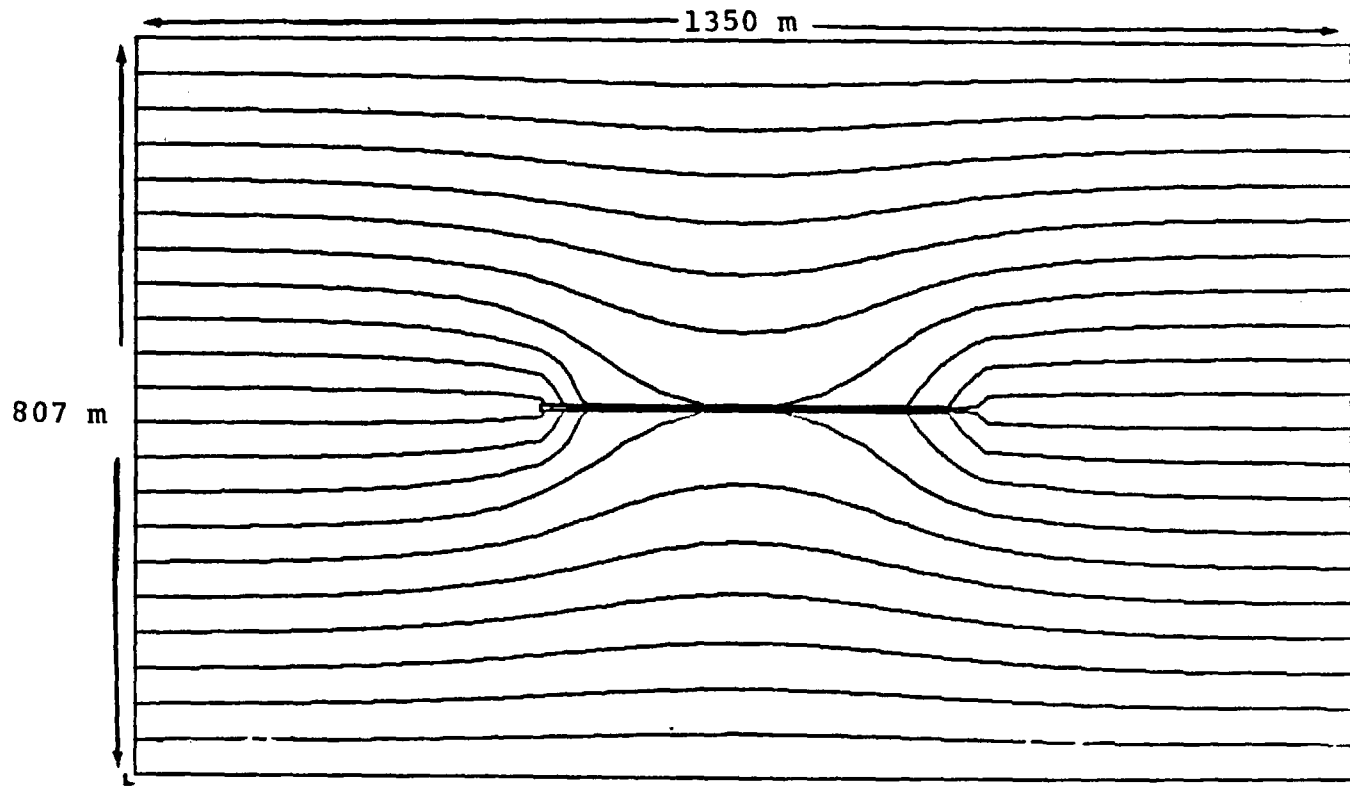


Figure 5. Isolated drift in saturated tuff ($k_{\text{rock}} = 10^{-15} \text{m}^2$) backfilled with material ($k_{\text{fill}} = 10^{-13} \text{m}^2$). Lines are evenly spaced streamlines resulting when a constant hydraulic gradient is held from left to right boundaries.

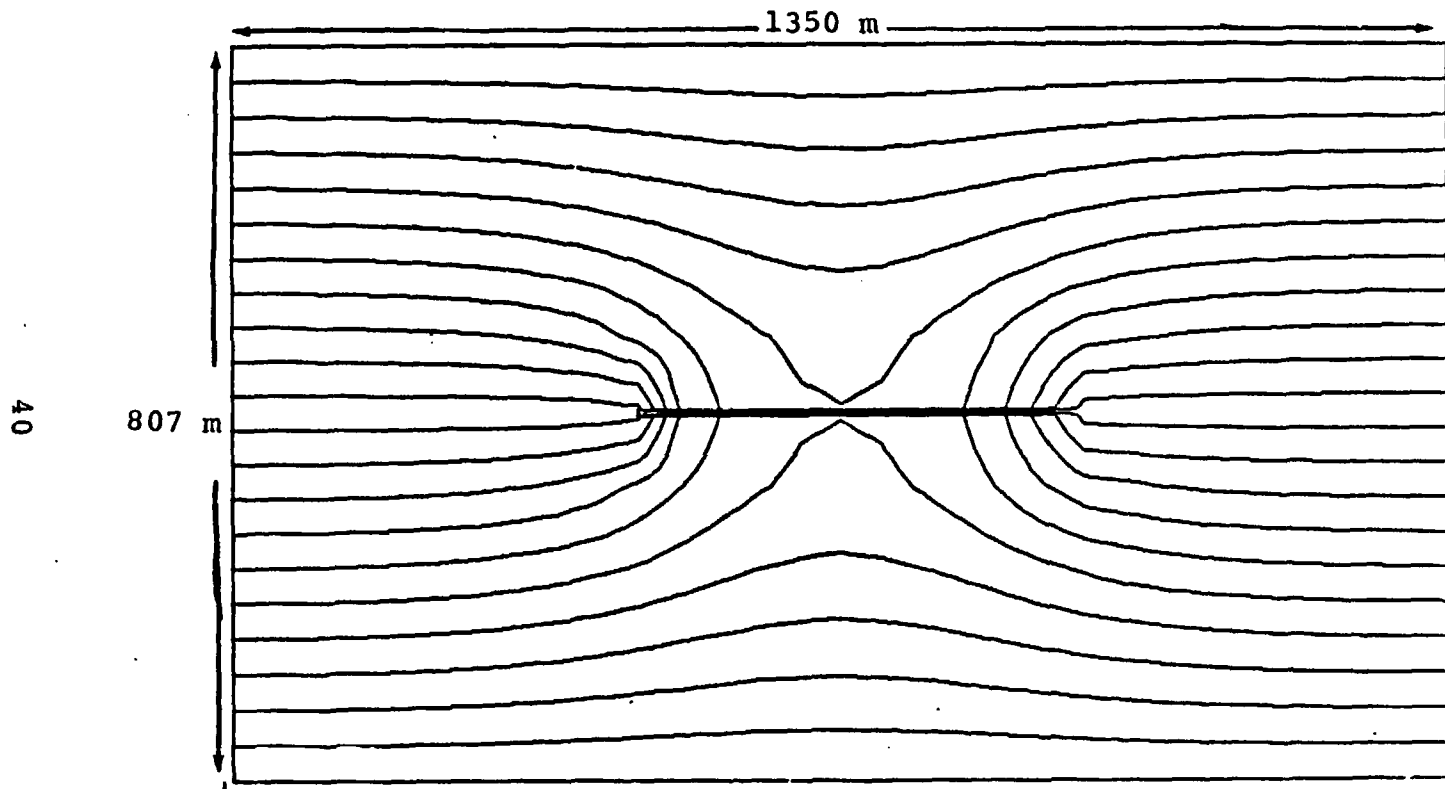


Figure 6. Isolated drift in saturated tuff ($k_{\text{rock}} = 10^{-15} \text{ m}^2$) backfilled with little material ($k_{\text{fill}} = 10^{-10} \text{ m}^2$). Lines are evenly spaced streamlines resulting when a constant hydraulic head is held from left to right boundaries.

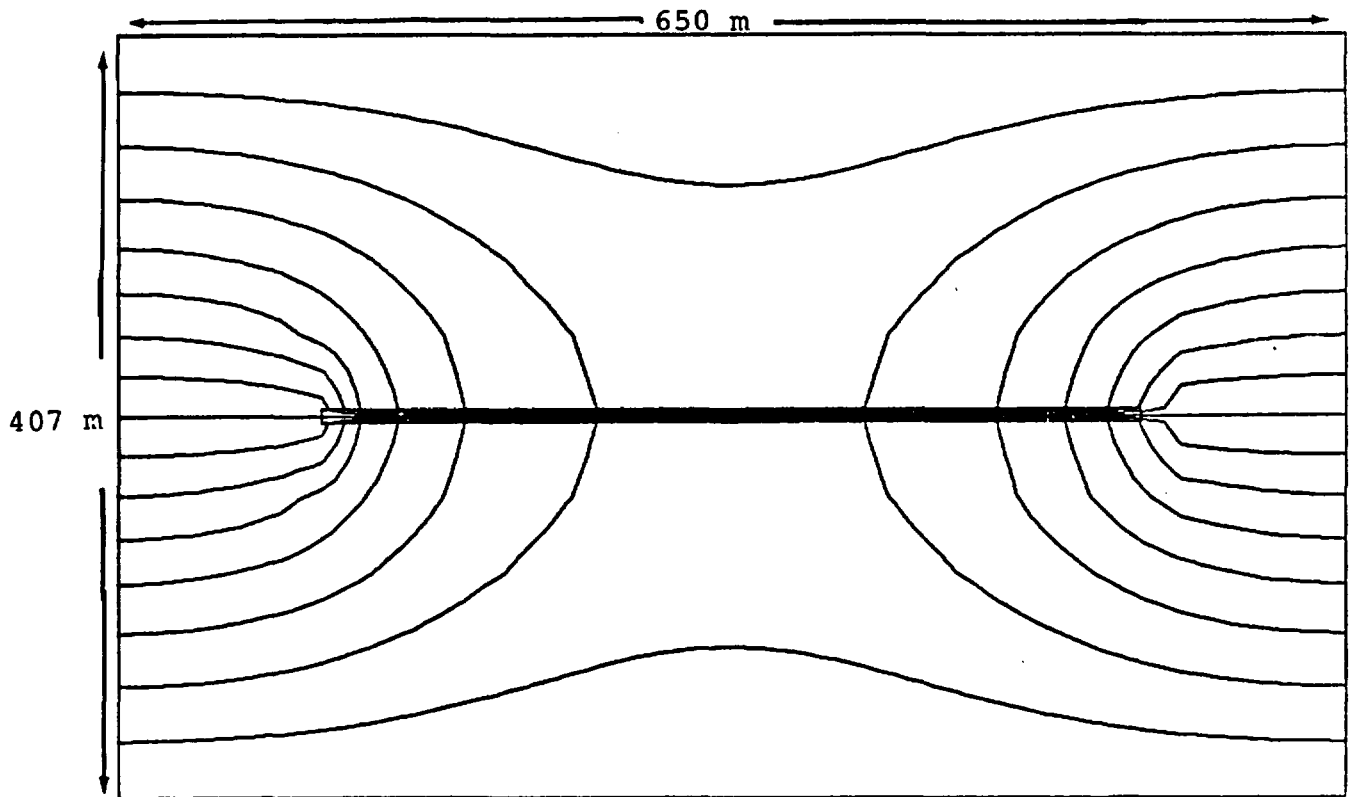


Figure 7. Isolated drift in saturated tuff ($k_{fill} = 10^{-10} m^2$) with boundary conditions prescribed 200 m from drift.

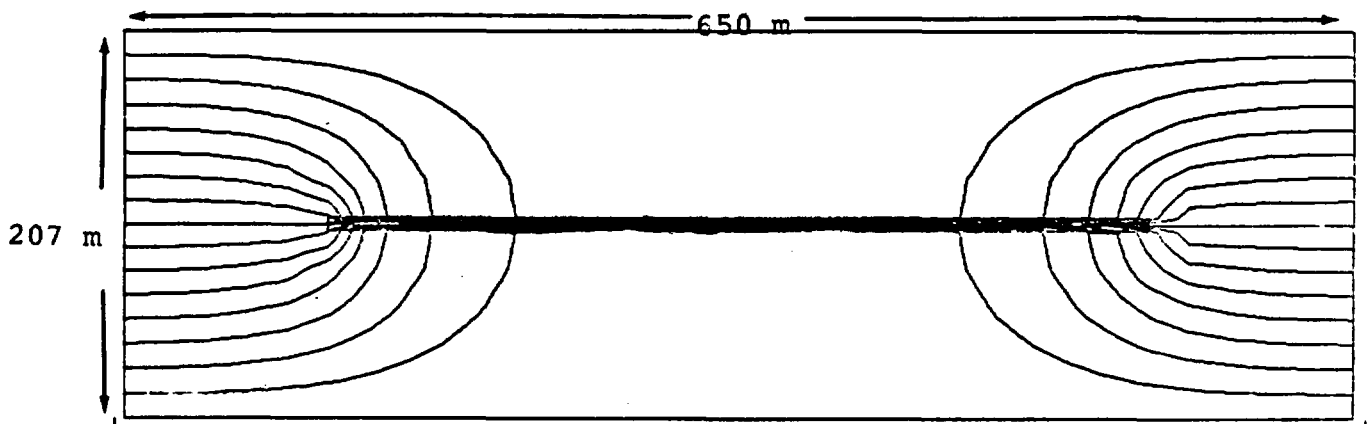


Figure 8. Isolated drift in saturated tuff ($k_{fill} = 10^{-10} m^2$) with boundary conditions prescribed 100 m from drift.

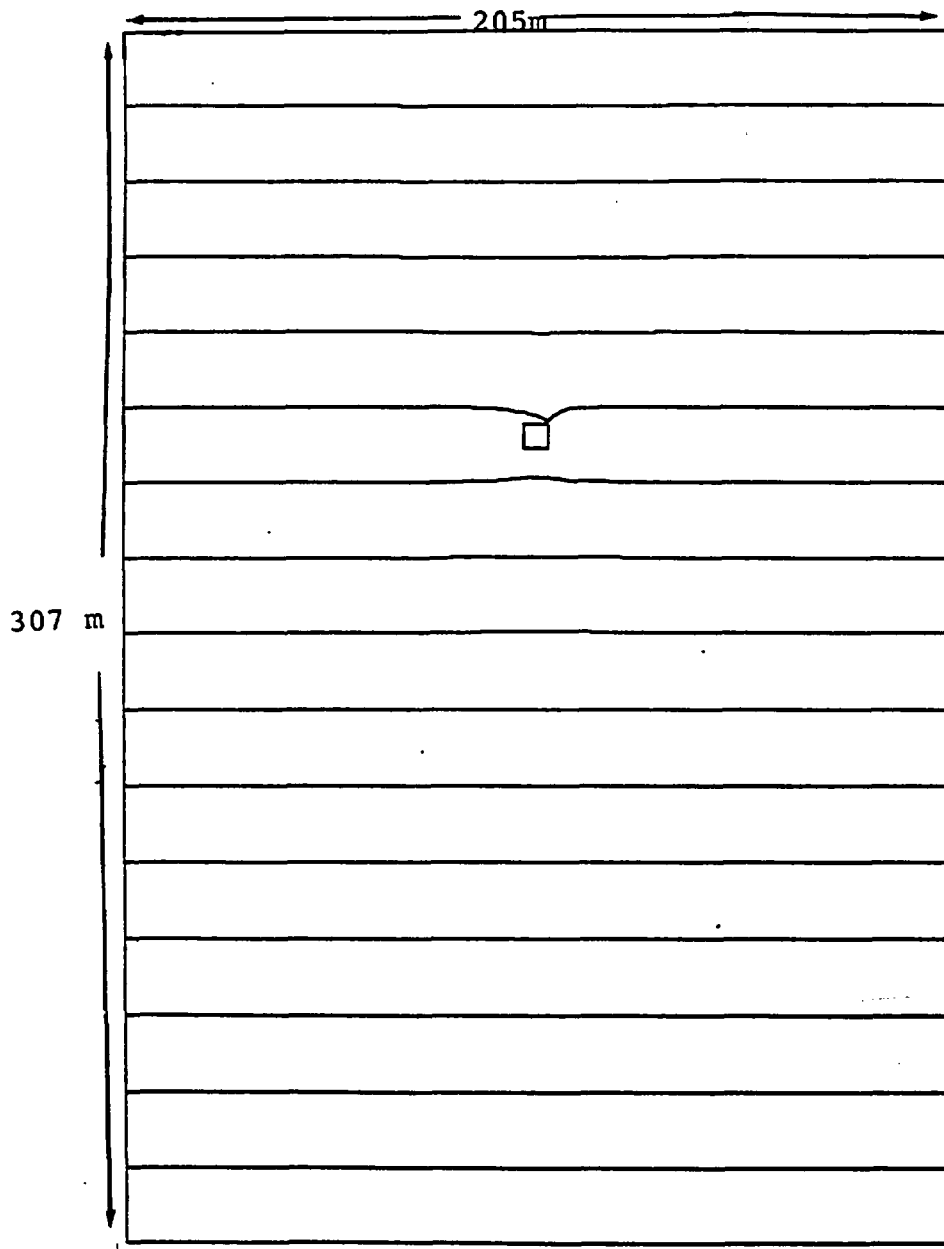


Figure 9. Cross-section of a 5m x 7m isolated drift ($k_{\text{fill}} = 10^{-10} \text{ m}^2$) in saturated tuff ($k_{\text{rock}} = 10^{-15} \text{ m}^2$). The drift is placed perpendicular to the flow resulting when a constant hydraulic gradient is applied from left to right boundaries.

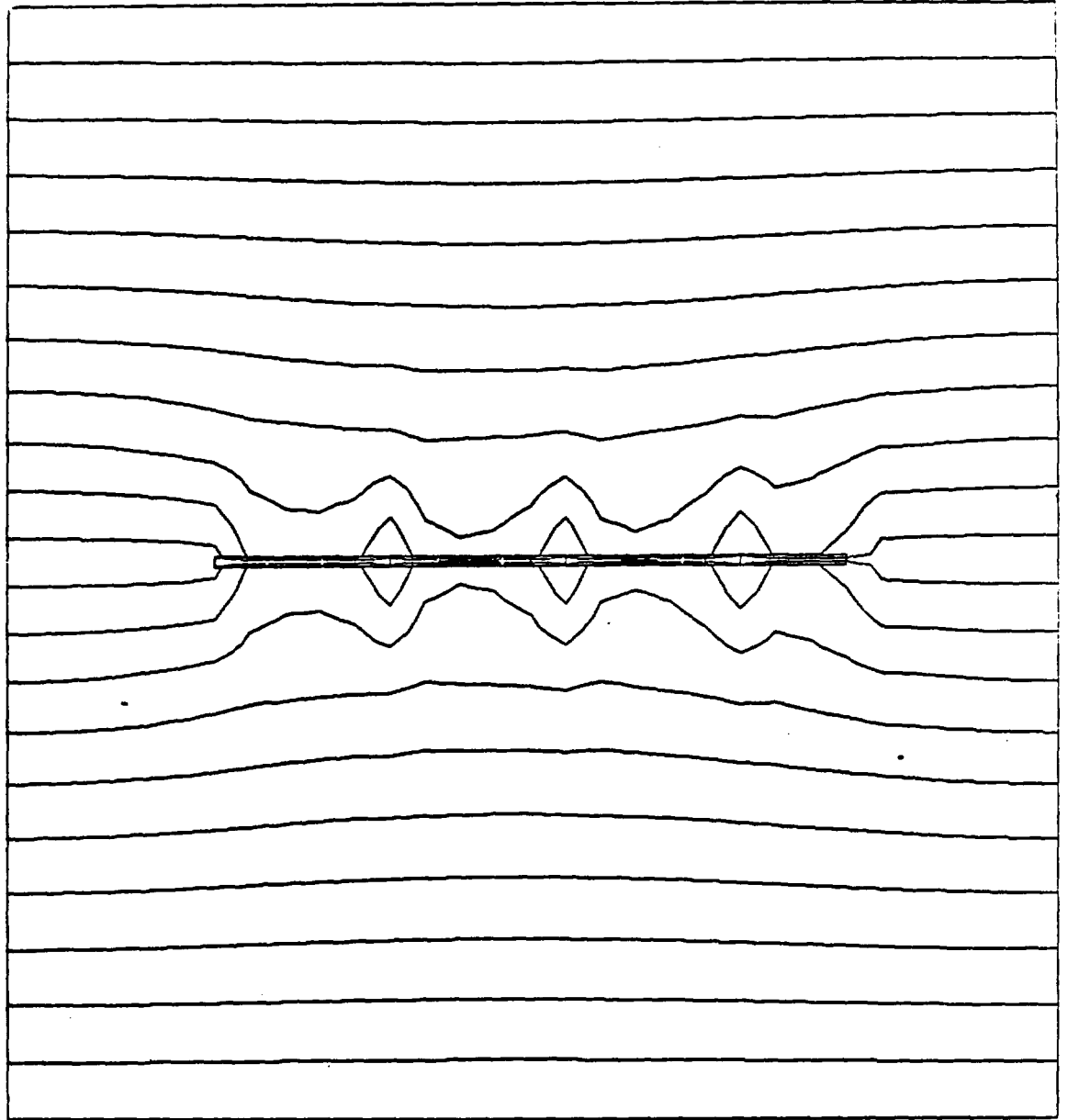


Figure 10. Flow through a drift with three 25m long, low permeability blocks ($k_{\text{block}} \approx k_{\text{rock}} = 10^{-15} \text{ m}^2$, $k_{\text{fill}} = 10^{-10} \text{ m}^2$). Lines are evenly spaced streamlines resulting when a constant hydraulic gradient is held from left to right boundaries.

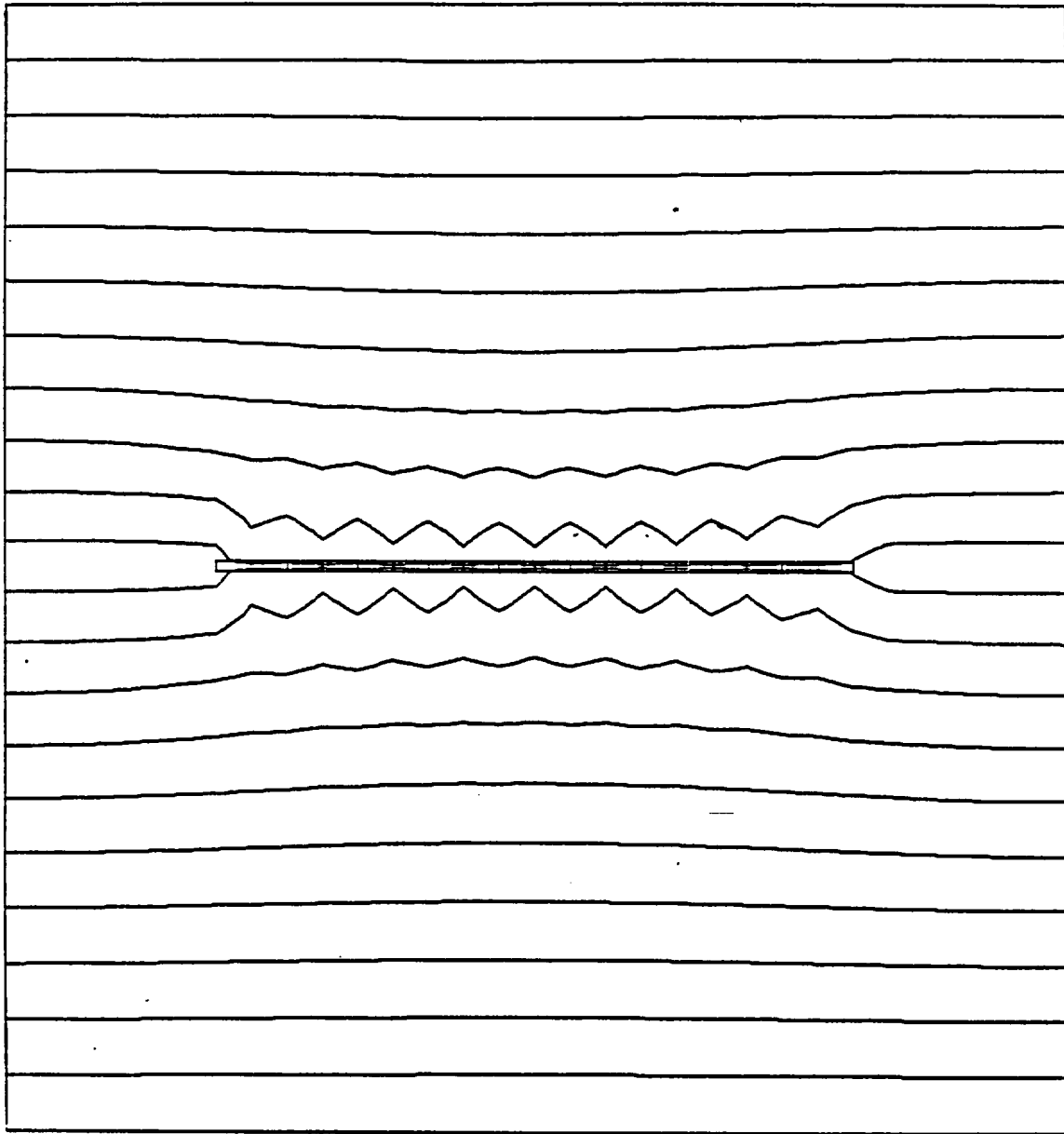


Figure 11. Flow through a drift with eight 25m long, low permeability blocks ($k_{\text{blocks}} \approx k_{\text{rock}} = 10^{-15} \text{ m}^2$, $k_{\text{fill}} = 10^{-10} \text{ m}^2$). Lines are evenly spaced streamlines resulting when a constant hydraulic gradient is held from left to right boundaries.

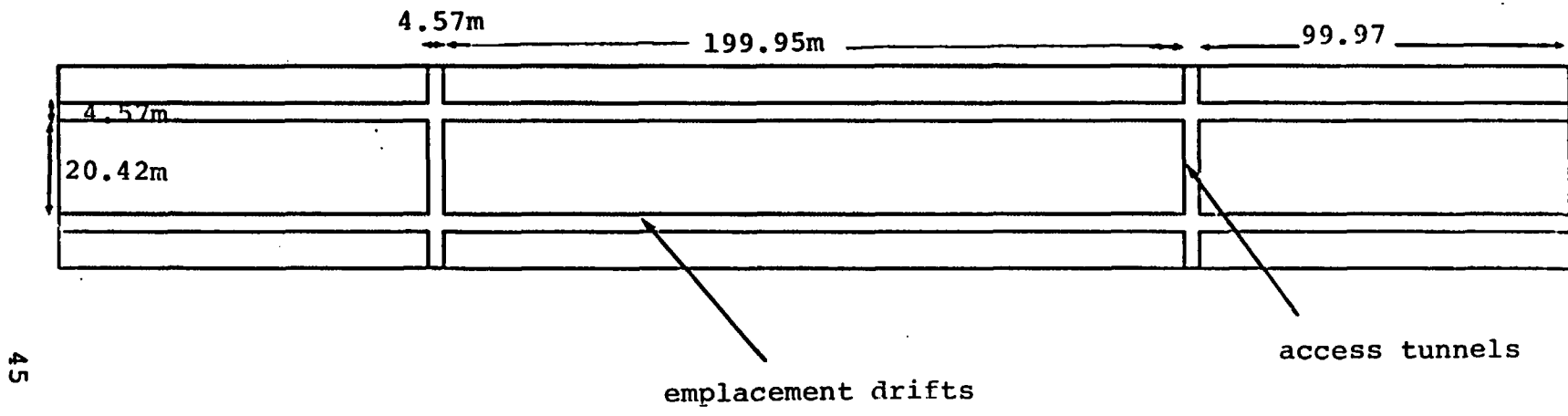


Figure 12. Plan view of vertical emplacement repository section.

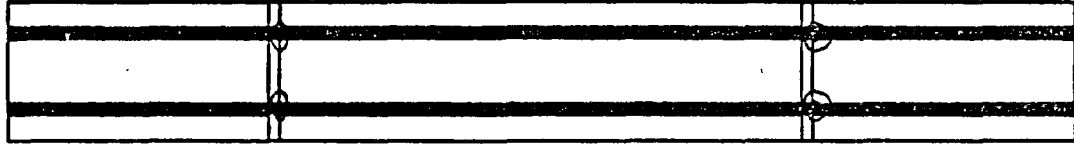


Figure 13. Flow through a repository with the emplacement drifts placed parallel to the hydraulic gradient; both access tunnels and emplacement drifts backfilled to $k_{fill} = 10^{-10} m^2$ ($k_{rock} = 8 \times 10^{-15} m^2$).



Figure 14. Flow through the undisturbed region.

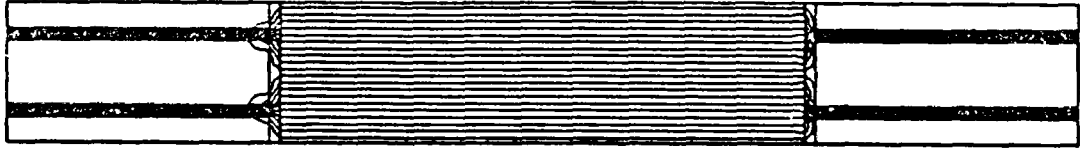


Figure 15. Flow through a repository with the drifts between some pairs of access tunnels backfilled to the rock permeability ($k = 8 \times 10^{-15} \text{m}^2$), the remaining have a permeability of 10^{-10}m^2 .

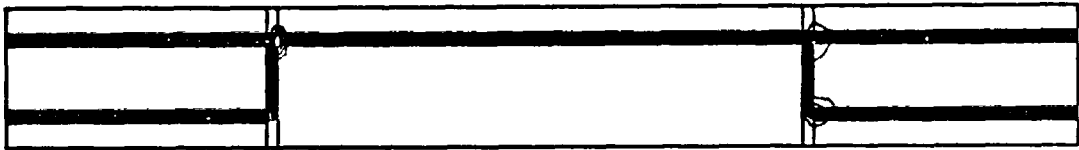


Figure 16. Flow through a repository with some emplacement drifts backfilled to rock permeability ($k = 8 \times 10^{-15} \text{m}^2$), while neighboring drifts are only loosely filled to $k = 10^{-10} \text{m}^2$.

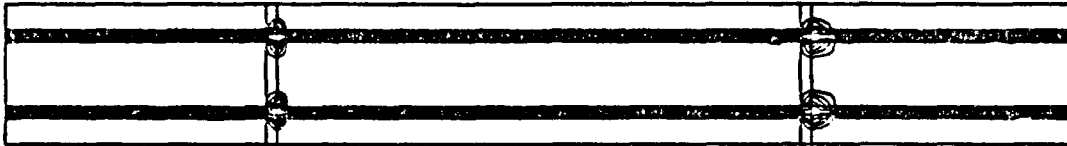


Figure 17. Flow through a repository, with junctions between drifts and access tunnels backfilled to rock permeability ($8 \times 10^{-15} \text{m}^2$). The drifts and tunnels themselves are backfilled to a permeability of 10^{-10}m^2 .

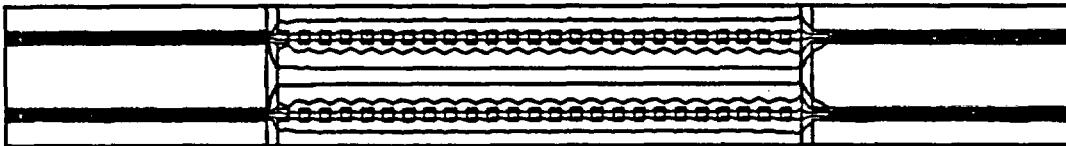


Figure 18. Flow through a repository with 4.0 meter blocks of rock permeability ($8 \times 10^{-15} \text{m}^2$) spaced 4.0 meters apart in emplacement drifts otherwise filled to only 10^{-10}m^2 in permeability.

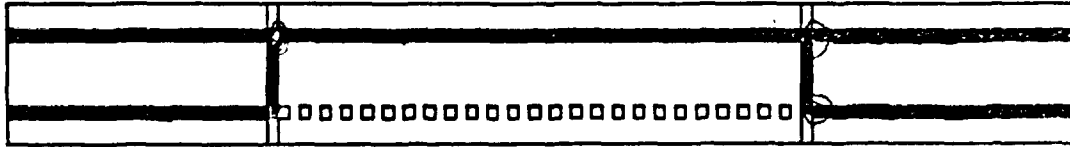


Figure 19. Flow through a repository with blocks ($k = 8 \times 10^{-15} \text{m}^2$) in an emplacement drift while a neighboring drift is only loosely backfilled ($k = 10^{-10} \text{m}^2$).

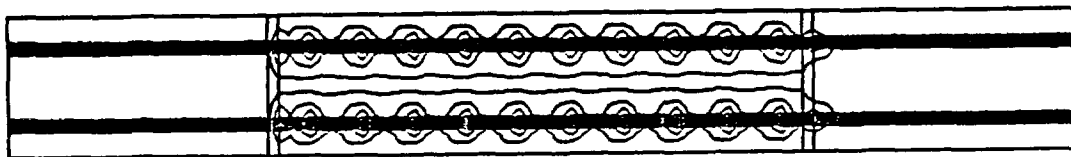


Figure 20. Flow through a repository with 4.0 meter blocks ($k = 8 \times 10^{-15} \text{m}^2$) spaced 16 meters apart in emplacement drifts otherwise backfilled to only 10^{-10}m^2 in permeability.

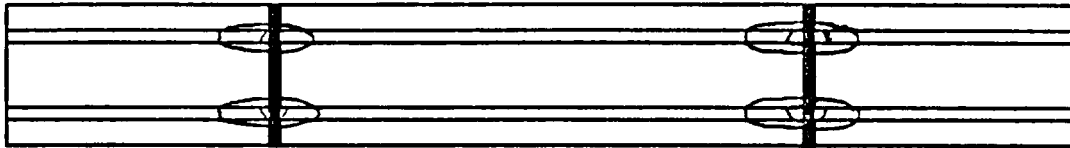
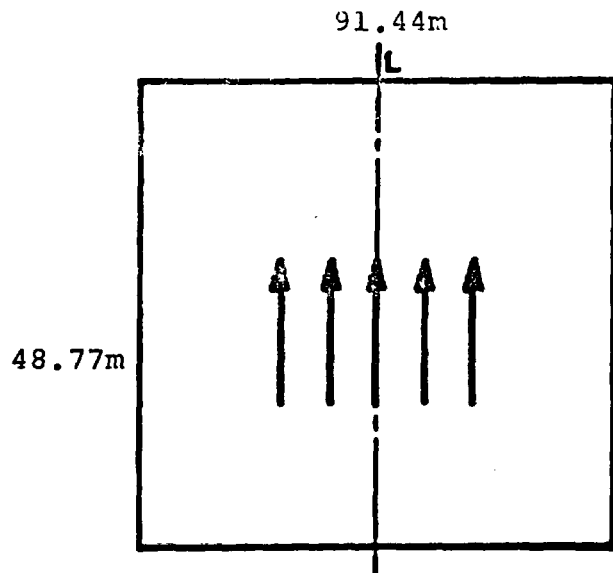
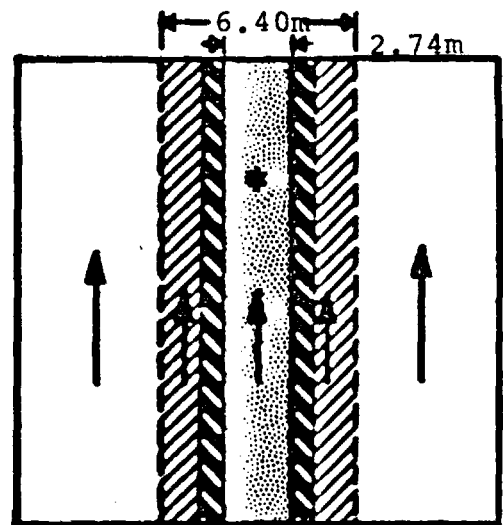


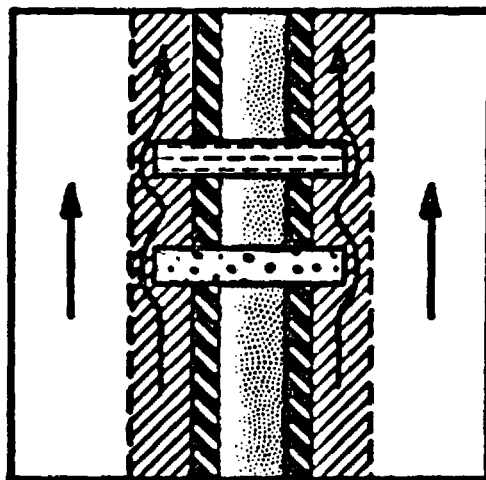
Figure 21. Flow through a repository positioned so that the dominant flow is parallel to access drifts. All drifts and tunnels are of permeability 10^{-10}m^2 , while the surrounding rock is of permeability $8 \times 10^{-15}\text{m}^2$.



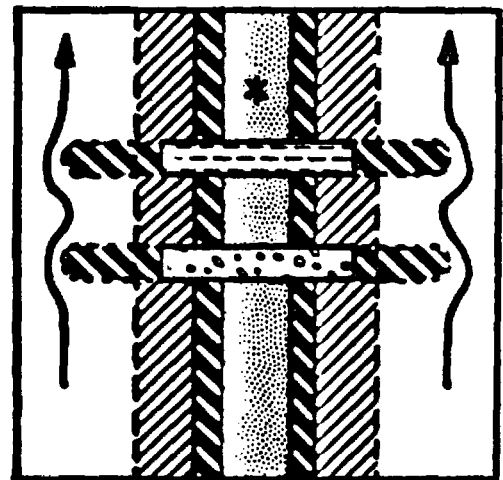
UNDISTURBED



MINIMAL SEAL



PRELIMINARY DESIGN



ENHANCED DESIGN

-  **CONCRETE**
-  **GROUT**
-  **CLAY**
-  **CRUSHED TUFF & CLAY**
-  **DISTURBED ZONE**

-  **CASE a. CRUSHED TUFF**
-  **CASE b. CRUSHED TUFF & CLAY**

Figure 22. Shaft studies

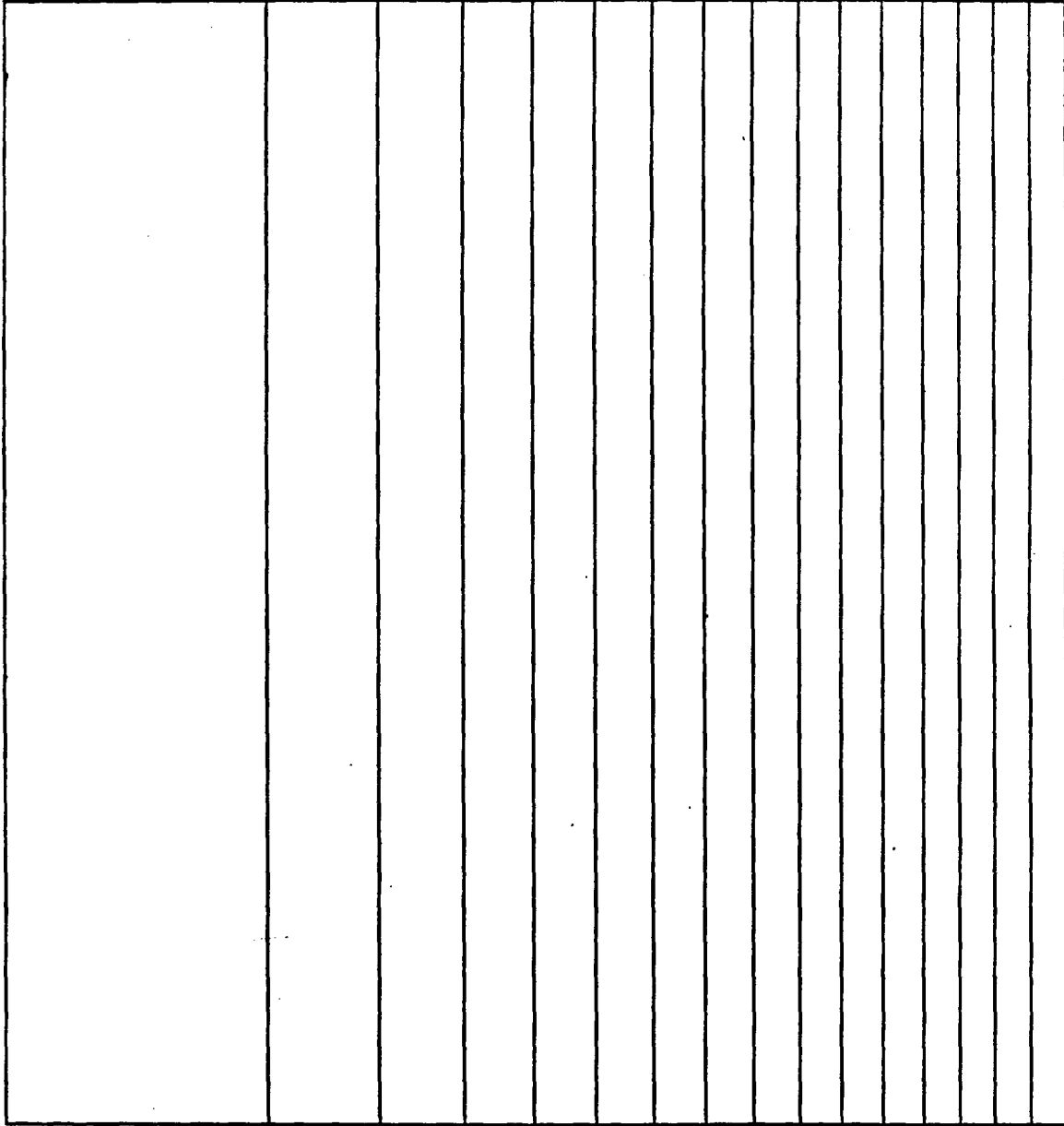


Figure 23. Vertical flow through undisturbed rock. Evenly spaced streamlines appear to become closer together to the right because of the axisymmetric geometry.

This dashed line represents both a material boundary and a coincident streamline.

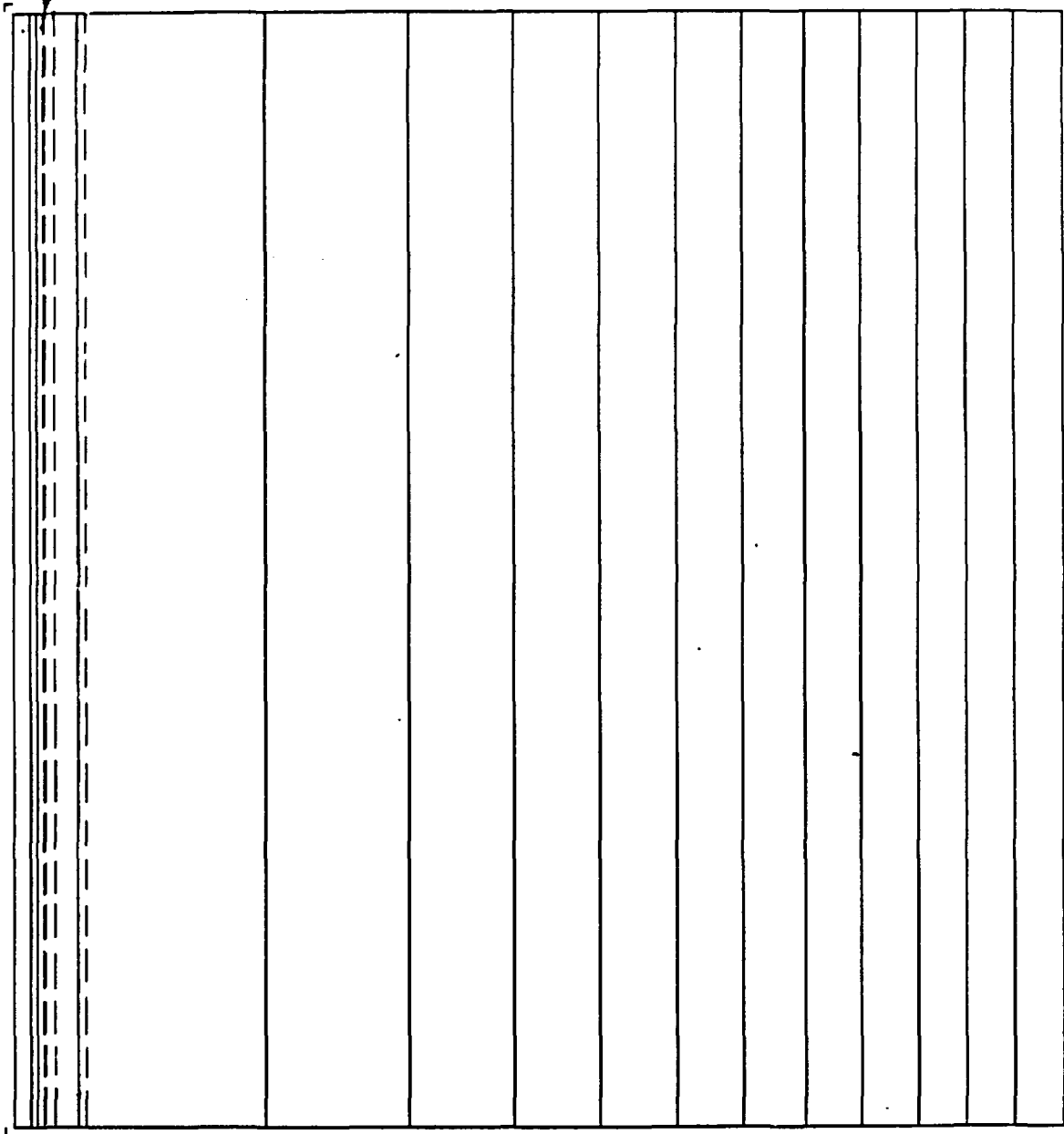


Figure 24. Vertical flow near a shaft with minimal seal, backfill of permeability $10^{-13}m^2$, grout and disturbed zone boundaries marked with dashed lines. Streamlines occur in the inner boundaries of the shaft, illustrating a much greater flow in this region than appeared in Figure 23.

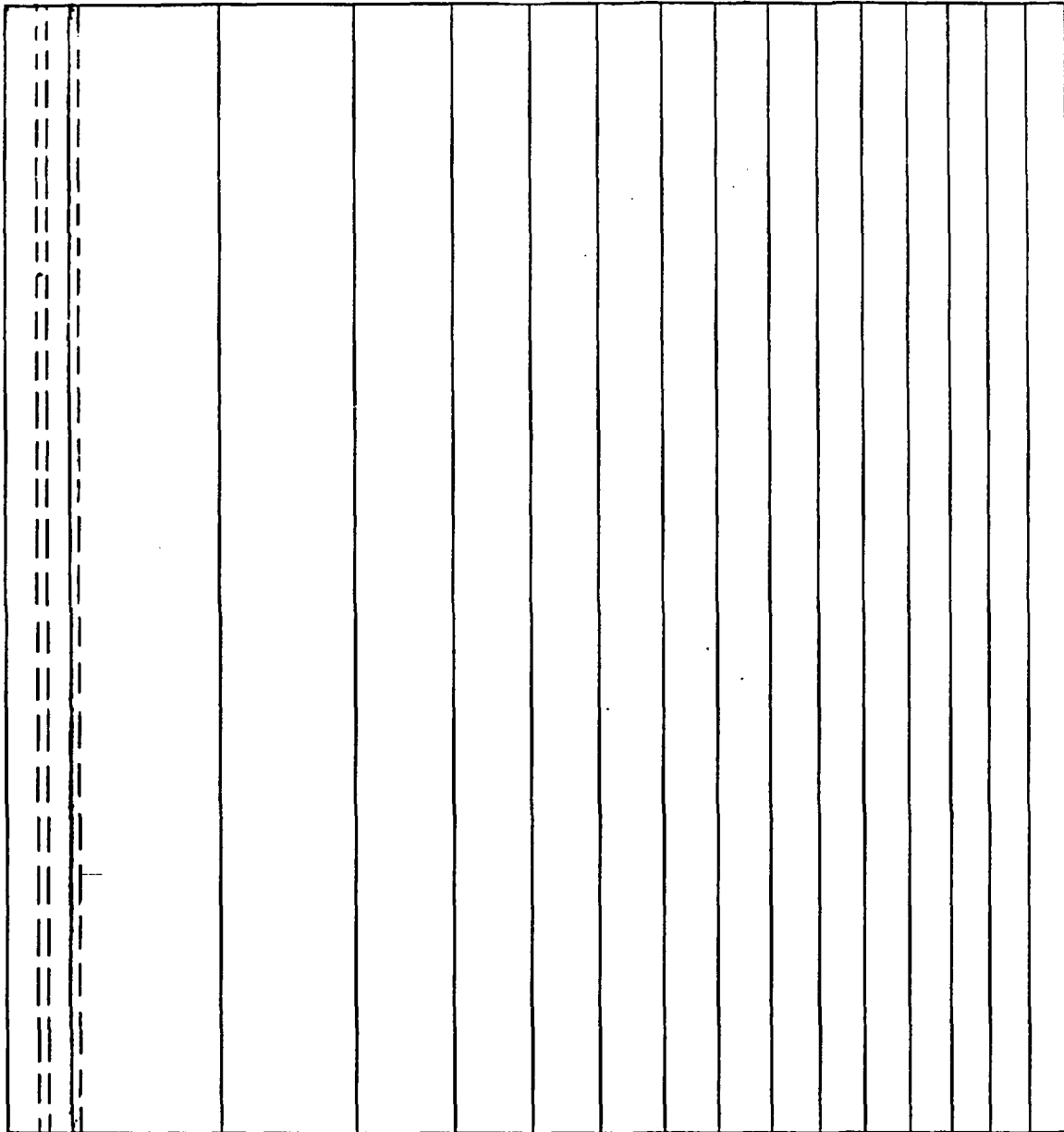


Figure 25. Vertical flow near a shaft with minimal seal; backfill of permeability $10^{-16}m^2$; grout and disturbed zone boundaries marked with dashed lines.

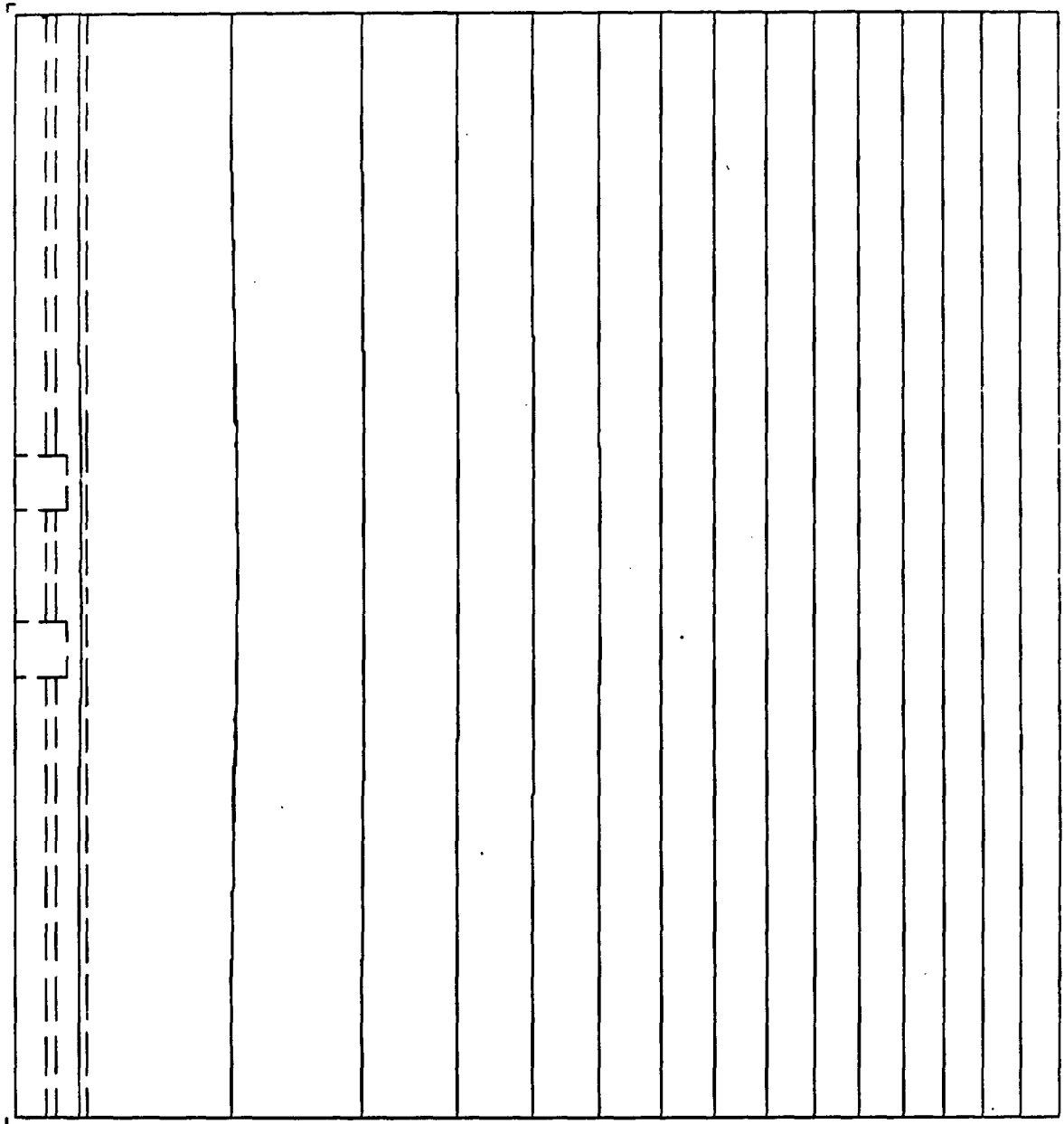


Figure 26. Vertical flow near a shaft with a clay and a concrete bulkhead in backfill of permeability 10^{-16}m^2 . Outline of shaft region is in dashed lines, while solid lines are equally spaced streamlines. Note that the streamlines vary little from those in Figure 25.

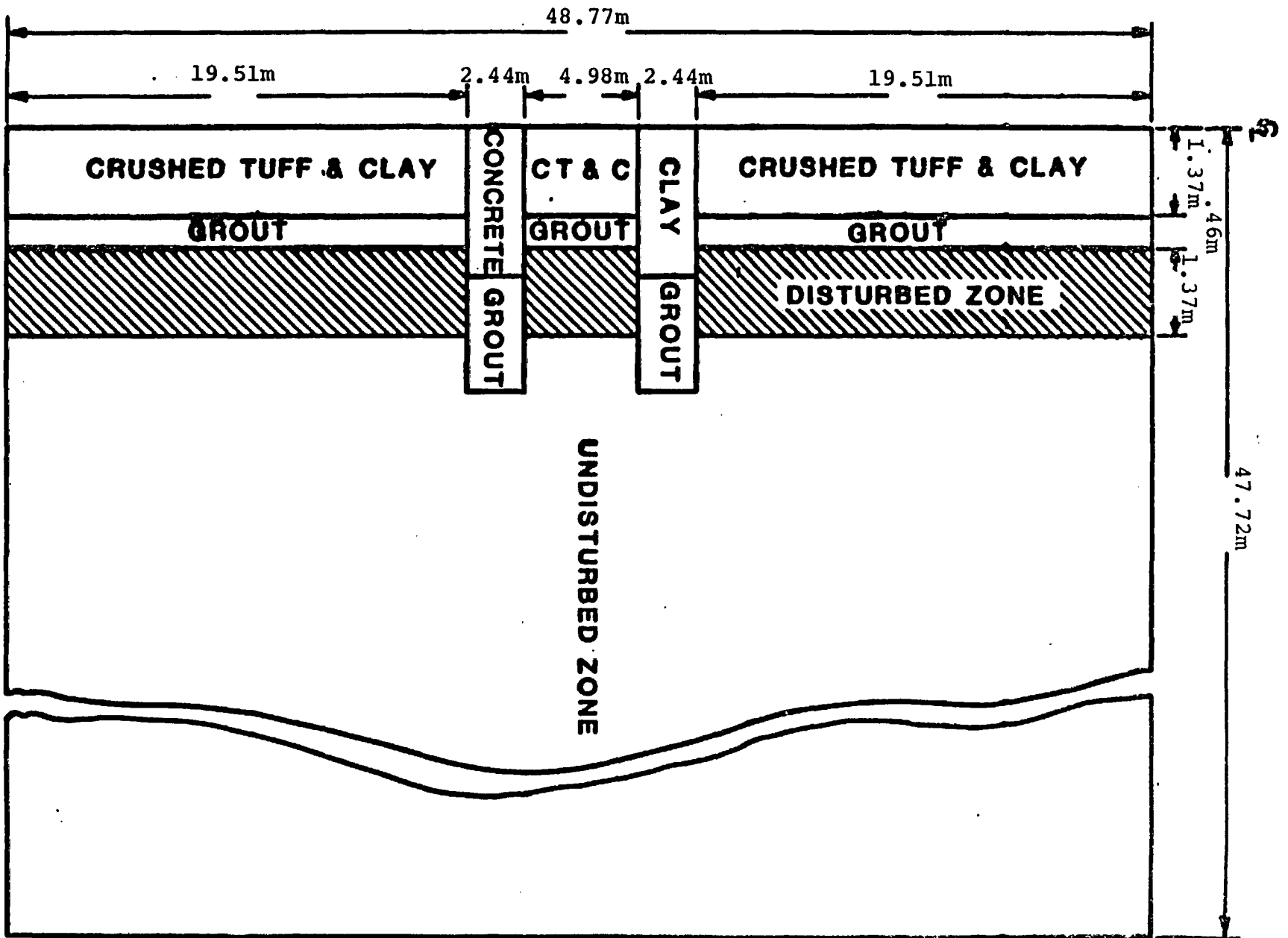


Figure 27. Enhanced seal design

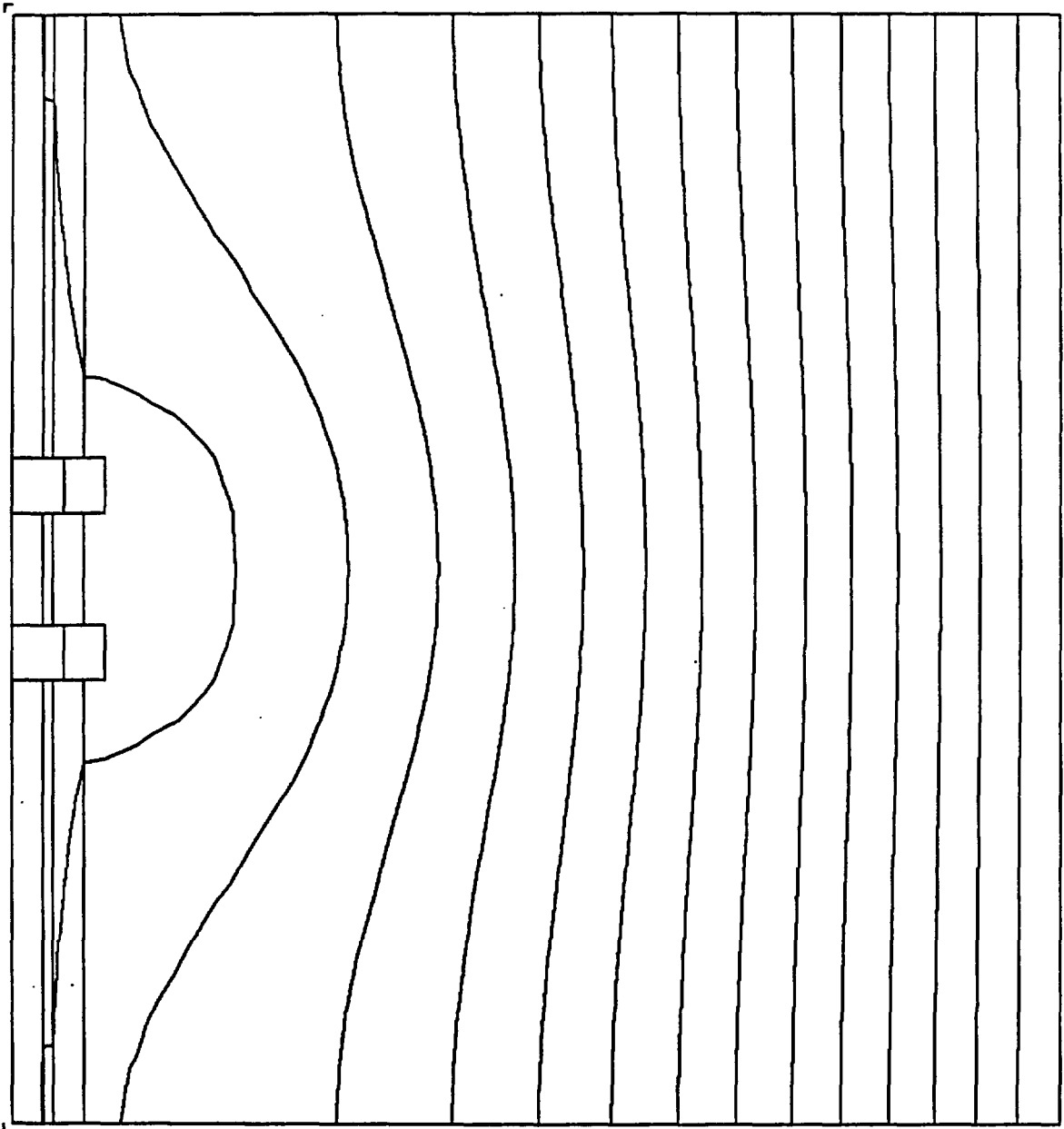


Figure 28. Flow near a shaft with the enhanced seal design; main shaft backfilled to permeability 10^{-13}m^2 .

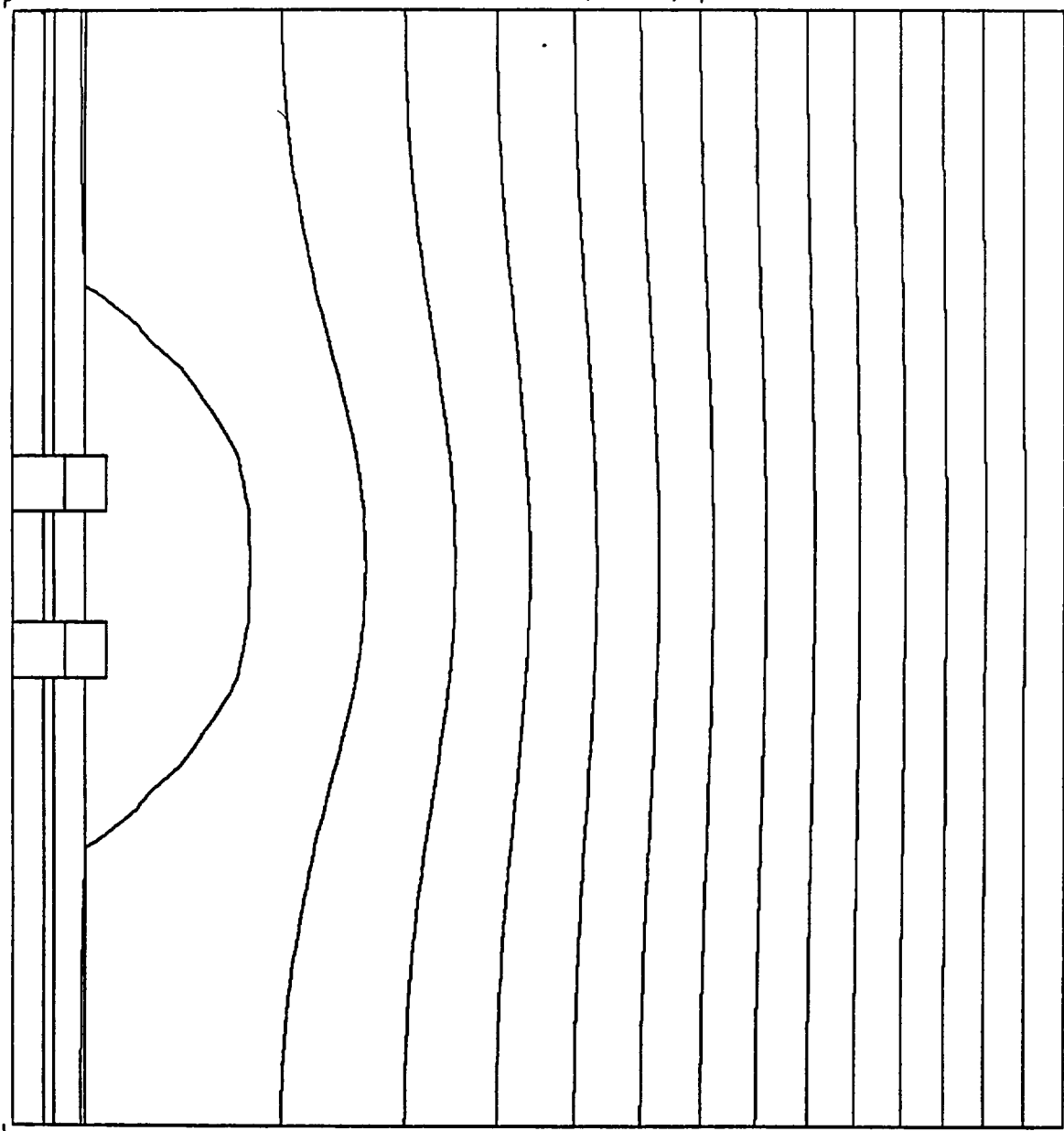


Figure 29. Flow near a shaft with the enhanced seal design; main shaft backfilled to permeability 10^{-16}m^2 .

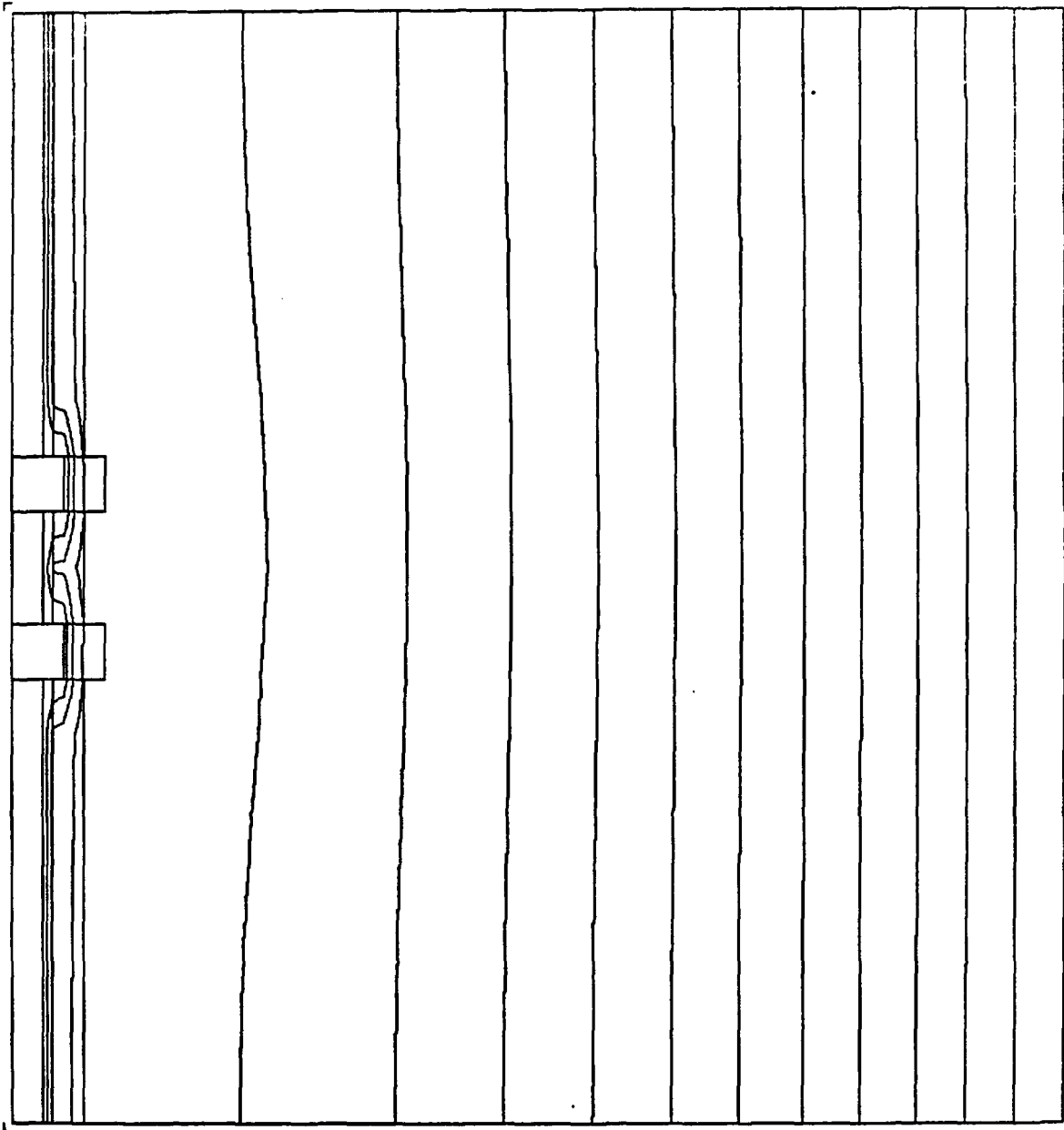


Figure 30. Flow near a shaft with the enhanced seal design, after 300 years (concrete and grout becoming more permeable).

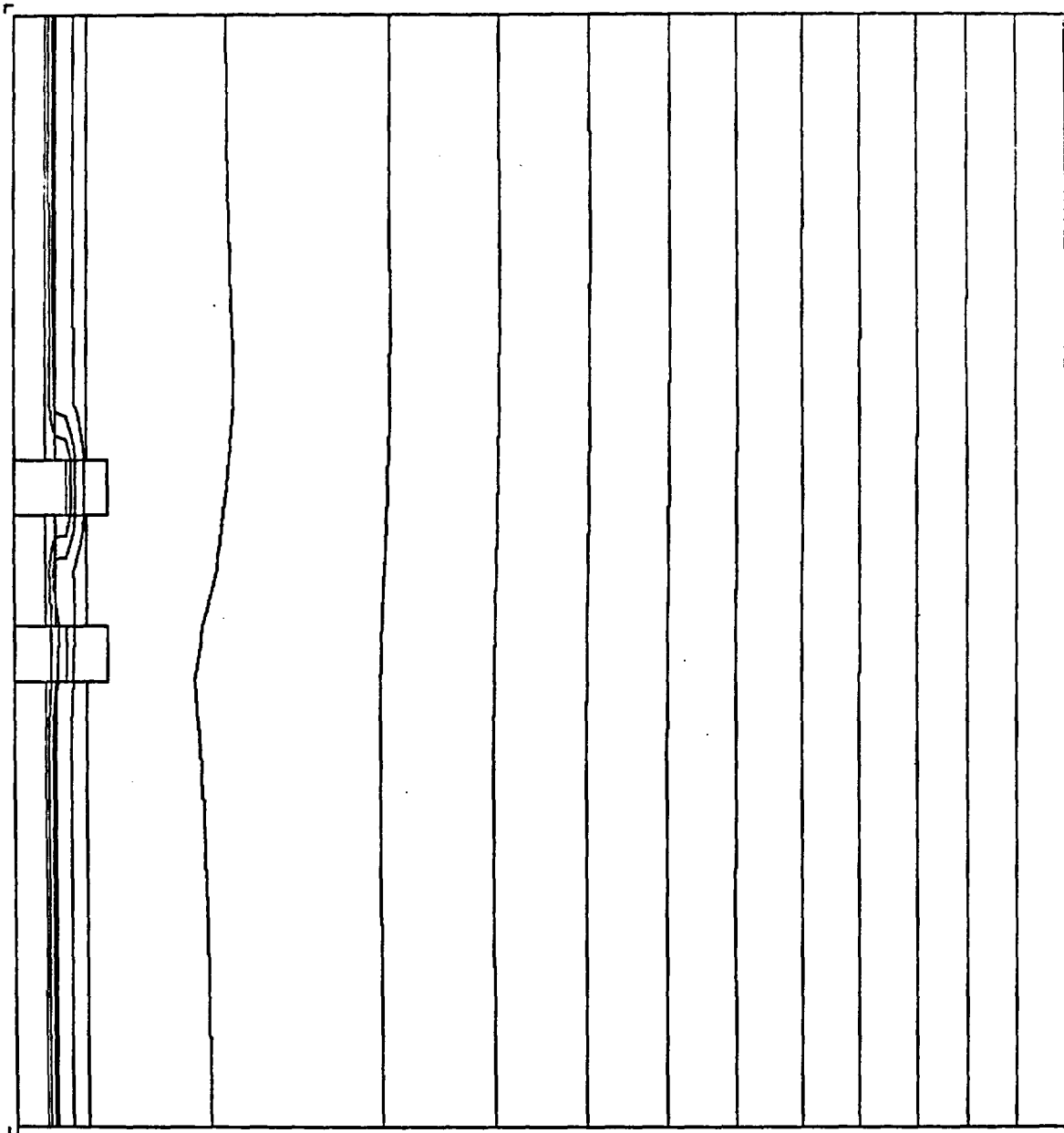


Figure 31. Flow near a shaft with enhanced seal design, after 3000 years (concrete becoming more permeable).

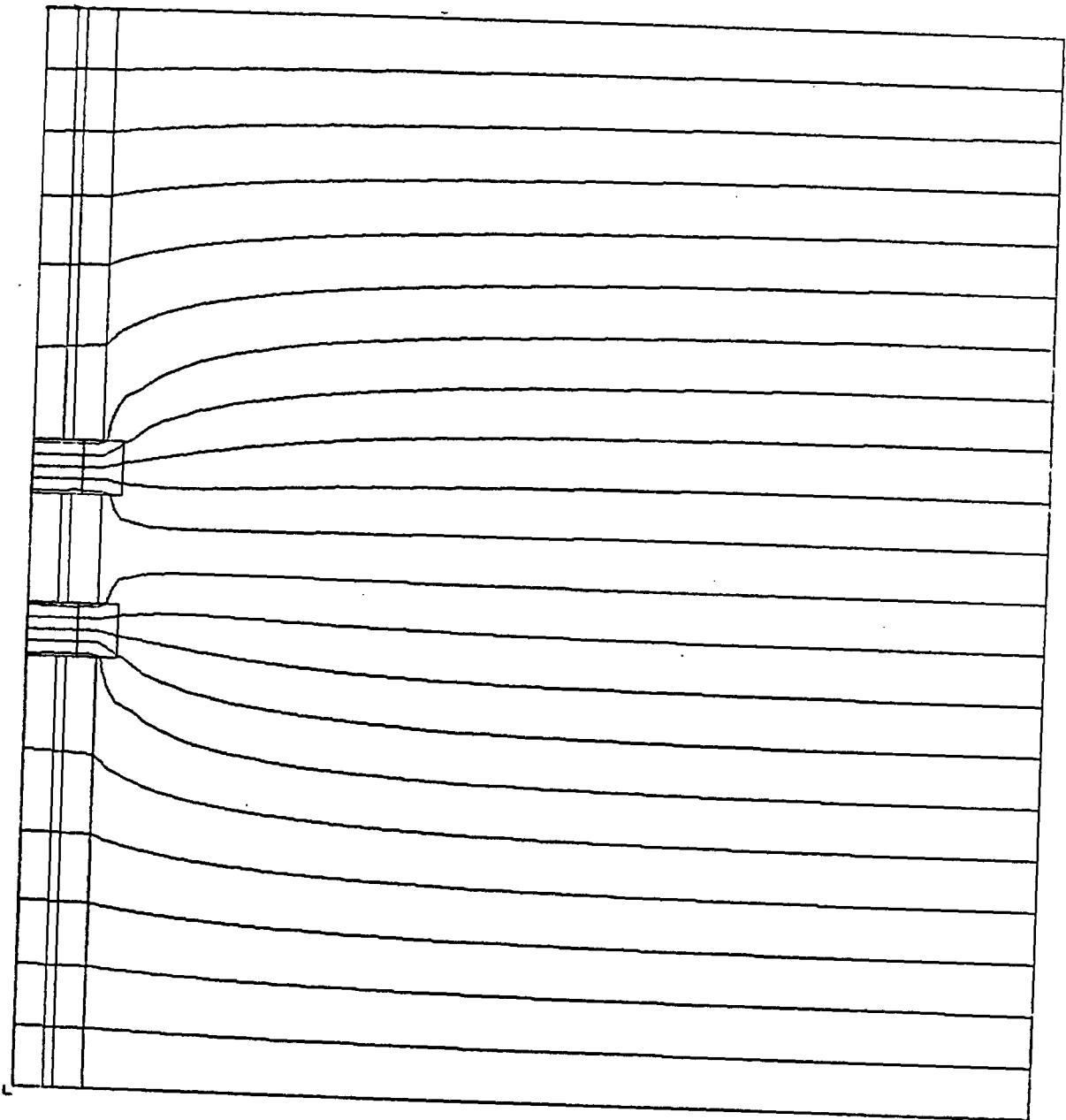


Figure 32. Constant-pressure lines for flow near a shaft with the enhanced seal design and backfill of permeability 10^{-16} m^2 . Constant-pressure boundary conditions along top and bottom boundaries.

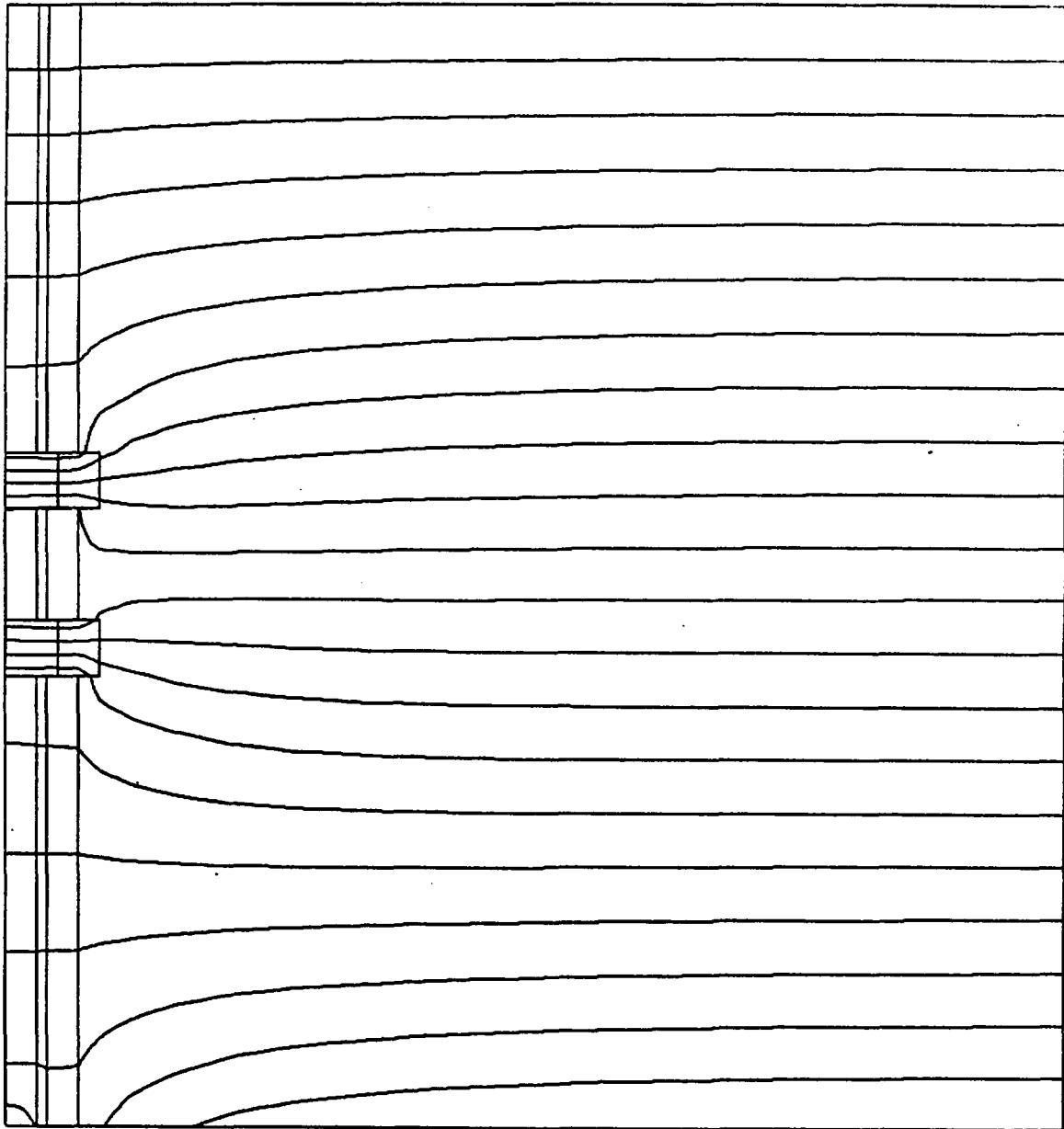


Figure 33. Constant-pressure lines for flow near a shaft with the enhanced seal and backfill of permeability 10^{-16}m^2 . The top boundary is constant pressure and the bottom is constant flow.

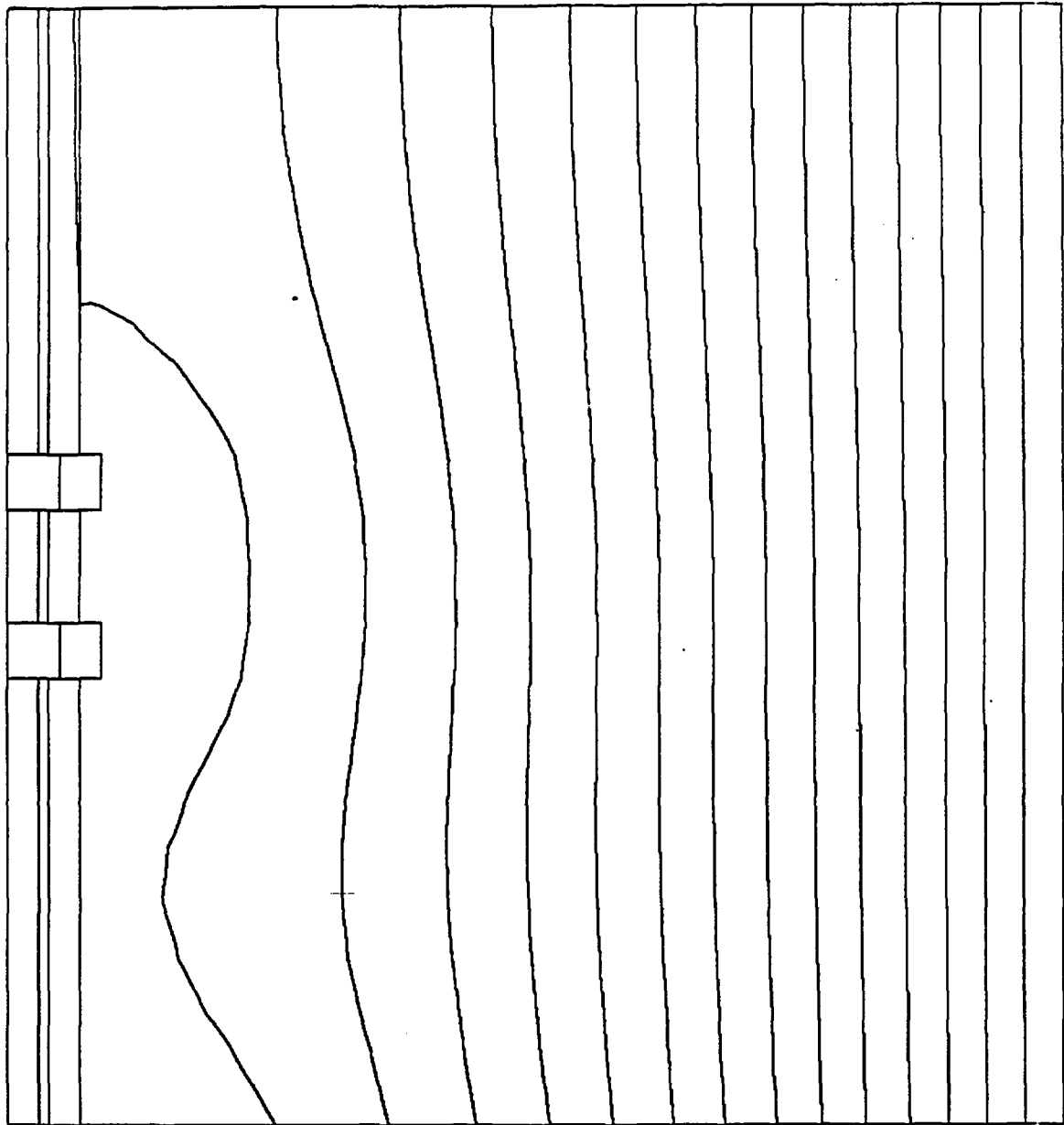


Figure 34. Streamlines near a shaft with the enhanced seal design and backfill of permeability 10^{-16} m^2 . The top boundary is constant pressure and the bottom is constant flow, as in Figure 33.

DISTRIBUTION:
Unlimited Release
UC-70

J. W. Bennett, Director
Geologic Repository Division
U.S. Department of Energy
NE-22
Washington, DC 20545

M. W. Frei
Geologic Repository Division
U.S. Department of Energy
NE-22
Washington, DC 20545

C. R. Cooley
Geologic Repository Division
U.S. Department of Energy
NE-22
Washington, DC 20545

C. H. George
Geologic Repository Division
U.S. Department of Energy
NE-22
Washington, DC 20545

J. J. Fiore
Geologic Repository Division
U.S. Department of Energy
NE-22
Washington, DC 20545

J. G. Vlahakis
Geologic Repository Division
U.S. Department of Energy
NE-22
Washington, DC 20545

T. P. Longo
Geologic Repository Division
U.S. Department of Energy
NE-22
Washington, DC 20545

C. Klingsberg
Geologic Repository Division
U.S. Department of Energy
NE-22
Washington, DC 20545

NTS Project Manager
High-Level Waste Technical
Development Branch
Division of Waste Management
U.S. Nuclear Regulatory Commission
Washington, DC 20555

Chief, High-Level Waste Technical
Development Branch
Division of Waste Management
U.S. Nuclear Regulatory Commission
Washington, DC 20555

J. O. Neff, Program Manager
National Waste Terminal
Storage Program Office
U.S. Department of Energy
505 King Avenue
Columbus, OH 43201

N. E. Carter
Battelle
Office of Nuclear Waste Isolation
505 King Avenue
Columbus, OH 43201

ONWI Library (5)
Battelle
Office of Nuclear Waste Isolation
505 King Avenue
Columbus, OH 43201

O. L. Olson, Project Manager
Basalt Waste Isolation Project
Office
U.S. Department of Energy
Richland Operations Office
Post Office Box 550
Richland, WA 99352

R. Deju
Rockwell International Atomics
International Division
Rockwell Hanford Operations
Richland, WA 99352

DISTRIBUTION:
Unlimited Release
UC-70

Governor's Office Planning
Coordinator
Nevada State Planning Coordination
State Capitol Complex, Second Floor
Carson City, NV 89710

J. I. Barnes, Director
Department of Energy
State of Nevada
400 W. King St., Suite 106
Carson City, NV 89710

K. Street, Jr.
Lawrence Livermore National
Laboratory
Mail Stop L-209
P.O. Box 808
Livermore, CA 94550

L. D. Ramspott
Technical Project Office
Lawrence Livermore National
Laboratory
P.O. Box 808
Mail Stop L-204
Livermore, CA 94550

D. C. Hoffman
Los Alamos National Laboratory
P.O. Box 1663
Mail Stop E-515
Los Alamos, NM 87545

D. T. Oakley
Technical Project Officer
Los Alamos National Laboratory
P.O. Box 1663
Mail Stop F-671
Los Alamos, NM 87545

W. W. Dudley, Jr.
Technical Project Officer
U.S. Geological Survey
P.O. Box 25046
Mail Stop 418
Federal Center
Denver, CO 80225

R. W. Lynch
Technical Project Officer
Sandia National Laboratories
P.O. Box 5800
Organization 9760
Albuquerque, NM 87185

G. F. Rudolfo
Technical Project Officer
Sandia National Laboratories
P.O. Box 5800
Organization 7254
Albuquerque, NM 87185

A. E. Stephenson
Sandia National Laboratories
P.O. Box 14100
Organization 9764
Las Vegas, NV 89114

D. L. Vieth, Director (5)
Waste Management Project Office
U.S. Department of Energy
P.O. Box 14100
Las Vegas, NV 89114

D. F. Miller, Director
Office of Public Affairs
U.S. Department of Energy
P.O. Box 14100
Las Vegas, NV 89114

D. A. Nowack (8)
U.S. Department of Energy
P.O. Box 14100
Las Vegas, NV 89114

B. W. Church, Director
Health Physics Division
U.S. Department of Energy
P.O. Box 14100
Las Vegas, NV 89114

A. E. Gurrola
Holmes & Narver, Inc.
P.O. Box 14340
Las Vegas, NV 89114

DISTRIBUTION:
Unlimited Release
UC-70

W. S. Twenhofel
820 Estes Street
Lakewood, CO 80215

H. D. Cunningham
Reynolds Electrical &
Engineering Company, Inc.
P.O. Box 14400
Mail Stop 555
Las Vegas, NV 89114

J. A. Cross
Fenix & Scisson, Inc.
P.O. Box 15408
Las Vegas, NV 89114

R. H. Marks
U.S. Department of Energy
CP-1, M/S 210
P.O. Box 14100
Las Vegas, NV 89114

A. R. Hakl, Site Manager
Westinghouse - AESD
P.O. Box 708
Mail Stop 703
Mercury, NV 89023

M. Spaeth
Science Applications, Inc.
2769 South Highland Drive
Las Vegas, NV 89109

G. Tomsic
Utah Dept. of Community
Economic Development
Room 6290, State Office Bldg.
Salt Lake City, UT 89114

U.S. Department of Energy (2)
Technical Information Center
P.O. Box 62
Oak Ridge, TN 37830

DISTRIBUTION:
Unlimited Release
UC-70

1510 D. B. Hayes
1511 J. W. Nunziato
1511 M. J. Martinez
1511 R. K. Wilson
1512 J. C. Cummings
1512 L. A. Mondy (8)
1513 D. W. Larson
1520 T. B. Lane
1521 R. D. Krieg
1524 W. N. Sullivan
1530 L. W. Davison
1540 W. C. Luth
7417 F. W. Muller
8120 L. D. Bertholf
9730 W. D. Weart
9760 R. W. Lynch
9761 L. W. Scully
9761 A. J. Mansure
9762 L. D. Tyler
9762 J. K. Johnstone
9762 J. P. Brannen
9762 R. R. Peters
9762 N. K. Hayden
9762 Y. T. Lin
9763 J. R. Tillerson
9763 R. M. Zimmerman
9763 J. A. Fernandez (5)
3214 M. A. Pound
3141 L. J. Erickson (5)
3151 W. L. Garner (3)
for DOE/TIC

DOE/TIC (25)
(C. H. Dalin, 3154-3)